Static and Fatigue Failure behavior of Aluminum Honeycomb Sandwich Structures subjected to three point bending loading

By:

MUZAMIL HUSSAIN

18-FET/MSME/S14

Supervised By:

DR. RAFIULLAH KHAN

DEPARTMENT OF MECHANICAL ENGINEERING,

FACULTY OF ENGINEERING AND TECHNOLOGY

INTERNATIONAL ISLAMIC UNIVERSITY,

ISLAMABAD.

Materials - Fatigue.
Aeronautics
Flexur & rigidity.

Thesis entitled

Static and Fatigue Failure behavior of Aluminum Honeycomb Sandwich Structures subjected to three point bending loading

Submitted to International Islamic University, Islamabad

In partial fulfillment of the requirements

for the award of degree of

MASTER OF SCIENCE

IN

MECHANICAL ENGINEERING

BY

Muzamil Hussain

18-FET/MSME/S14

SESSION 2014-2016

DEPARTMENT OF MECHANICAL ENGINEERING

INTERNATIONAL ISLAMIC UNIVERSITY,

ISLAMABAD

DECLARATION

I, **Mr. Muzamil Hussain**, Reg. No. **18-FET/MSME/S14** student of MS mechanical engineering in Session 2014-2016, certify that research work titled "Static and Fatigue Failure behavior of Aluminum Honeycomb Sandwich Structures subjected to three-point bending loading" is my own work. The work has not been presented elsewhere for assessment. Where material has been used from other sources it has been properly acknowledged.

Signature of student: 10/01/17

Dated: _____

Certificate of Approval

This is to certify that the work contained in this thesis entitled, **"Static and Fatigue Failure behavior of Aluminum Honeycomb Sandwich Structures subjected to three point bending loading"** was carried out by **Muzamil Hussain Registration# 18-FET/MSME/S14,** it is fully adequate in scope and quality, for the degree of MS (Mechanical Engineering).

Viva Voice Committee

Supervisor

Dr. Rafiullah Khan

Assistant Professor

DME, FET, IIU, Islamabad

10/01/2017

Internal Examiner

Dr. Saeed Badshah

Head of Department (HOD)

DME, FET, IIU, Islamabad

11/1/17

External Examiner

Dr. Riffat Asim Pasha

Head of Department (HOD)

Department of Mechanical Engineering

UET Taxila

11/01/17

Chairman DME FET IIU, Islamabad

12/01/17

Dean FET, IIU Islamabad

Prof. Dr. Aqdas Naveed Malik

DEDICATION

I would like to dedicate this research work to my honorable and generous family, respected teachers and friends specially my late father, Mr. Imdad Hussain and my mother. I also dedicate it to my brother, Mr. Sajid Hussain who trusted in me more than myself, loved me and cared for me unconditionally.

ACKNOWLEDGEMENTS

All praises belong to Almighty ALLAH who has bestowed me with good health and enlightened path that made me stand on my own today. Blessing on MOHAMMAD (S.A.W), the seal of the prophets and his pious progeny. I would like to present my gratitude to **Dr. Rafi Ullah Khan** who taught me the real meaning of Research through this journey. He is undoubtedly among the persons who can easily be a source of inspiration to anyone. I am really thankful for his kind supervision and firm believe in me that helped me in analyzing the problem and deriving its solution.

I would like to extend my gratitude in favor of Faculty of UET Taxila, specially Engr. Zaheer Abbas and Engr. Faisal Qayum, they always tried to convince me towards hard work and orientation of my goals. I am really grateful to them for counselling and troubleshooting. I would like to pay my special thanks to my friend Mr. Waseem Ur Rahman who helped me in preparing my thesis. Last but not the least, Engr. Mudasir Ijaz and Engr. Habib Ullah and Engr. Sherasim Niazi proved to be my true companions by consistently standing by my side. I am really very thankful to these friends of mine.

ABSTRACT

Honeycomb sandwich structures are composed of two thin face sheets and thick light weight core with adhesive. These structures are used in light weight applications especially in aeronautics, marine, vehicles and civil engineering industry because of the high flexural rigidity per unit weight. The static and fatigue failure behavior of honeycomb sandwich structures have been investigated in this paper. Under static loading, the load and mid span displacement response corresponds to four different phases. The fatigue life of the panel is evaluated by performing the constant amplitude loading at the several loading levels. The results show that fatigue life increases as the stress level decreases. The visual and optical analysis was performed to analyze static and fatigue failure. The fracture modes were analyzed using Scanning Electron Microscope (SEM). It was investigated that the sandwich structures subjected to three point bending load fail in various ways including face yield, core indentation, core shear failure and delamination at core and face sheet interface depending upon the loading conditions.

List of Figures

List of Tables

List of Abbreviations

ASTM: American Society for Testing and Materials

SEM: Scanning Electron Microscope

BS: Bending Stress

SS: Shear Stress

MTS: Material Testing System

HOSBT: High Order Sandwich Beam Theory

GFRP: Glass Fiber Reinforcement Plastic

CFRP: Carbon Fiber Reinforcement Plastic

PVC: Poly-Vinyl Chloride

PMI: Poly-Methacryl-Imide

PAN: Poly-Acrylonitrile

Chapter 1

INTRODUCTION

Composite materials are used as advanced materials in many areas such as aircraft and automobile industry where strength to weight ratio is one of the most significant design parameter. The new advancement in composite structures is sandwich structure that increases the structural efficiency to many times by fractional increase in weight and because the increase of bending stiffness per unit weight [1]. Composite Sandwich panels have a significant heat resistance, high resistant to corrosion and outstanding energy absorption abilities [2]. The introduction of composite sandwich structure, the failure modes of sandwich structure, objectives of research and research methodology is briefly discussed in this chapter.

1.1 Composite Sandwich Materials

Sandwich structure is formed by bonding a thin layer of high strength face-sheet to both side of the thick, light weight core [3] as shown in figure 1.1. Face-sheet are stiffer and stronger whereas core is light, flexible and less stiffer so when these are combined in sandwich structures they produced light weight structures that are used in aerospace and marine industry [4].

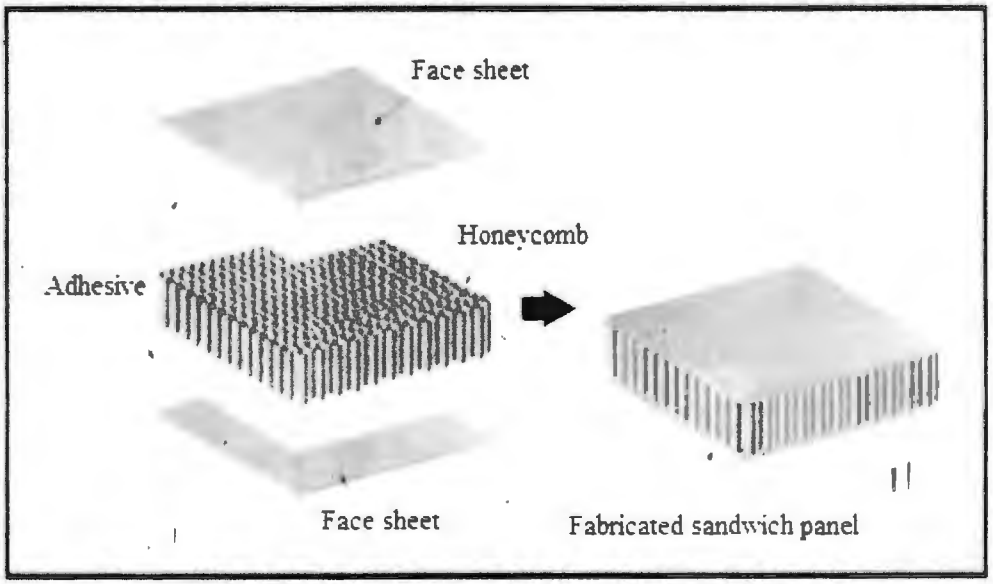

Figure 1.1: Sandwich structure [3]

The primary function of face-sheet is to resist the compression and tensile loading while the core is meant to resist transverse shear loads in addition to ensure the correct distance between the face-sheets and to avoid sliding with respect to each other. Sandwich structures are most of the time symmetric means the face-sheet on both side of the core is identical in thickness and materials. However in axisymmetric sandwich structures both the face-sheets are not identical either in thickness or in material. The use of core increases the moment of inertia of the sandwich structures with little increase in weight, thus making the sandwich structure ideal for light weight applications like aeronautical structures, racing cars and high speed marines [5]. The relative flexural strength of sandwich structures in terms of thickness and weight is given in table 1.1.

Table 1.1: Relative flexural strength of sandwich structures in terms of thickness [5]

Thickness of Panel			
Relative Bending Stiffness	1	7.0	37
Relative Bending Strength	1	3.0	9.2
Relative Weight	1	1.03	1.06

1.2 Constituents of Sandwich Structures

The composite sandwich panels consists of thin, stiffer face-sheets, thick light weight core and an adhesive. The strength and stiffness of sandwich structures mainly depends upon the types of materials used for facing and core [6]. The selection of materials is on the bases of high strength and stiffness under in plane compression, economic and environment considerations and thermal properties [7].

1.2.1 Face Sheets

The face sheet of sandwich structure can be made of fiber laminates, metal or any other composite laminates. A large number of face sheets are available that differ in certain properties. The most widely used face sheets are made of glass fibers, carbon fibers, aluminum metal or aluminum alloy [8]. Stainless steel, Aramid fibers, Plywood, Concrete, foam and flax are also used as a facing material.

1.2.2 Core

The core may be of made of any material but generally there are of four types; honeycomb core, web core, foam or solid core, corrugated or truss core [5, 9] as shown in figure 1.2. To increase the stiffness of core low shear modulus of materials are suitable that increases the deflection in case of bending stress. The core must be of low stiffness and it determine the flexural stiffness and compressive behavior of sandwich structure besides stabilizing the face sheets and complete panel [10, 11]. Honeycomb and corrugated truss core strongly increases the bending strength of sandwich panels [12] It is considered that for an optimum design the cross sectional area of cell should be very small to increase the number of cells in allowable length [13]. Aluminum, aramid fiber (Nomex HRH10), carbon fiber and foam are most widely materials that are used for core. Composite, Steel, wood, concrete and glass fiber is also used as a core material.

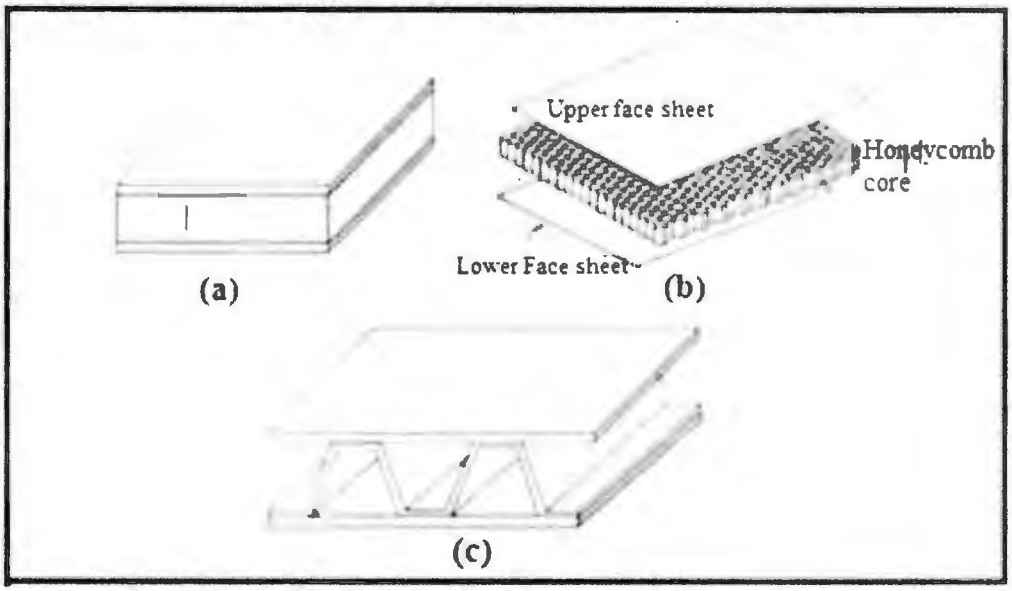

Figure 1.2: Core configurations. (a) Foam core (b) Honeycomb core (c) Corrugated core [9]

1.2.3 Adhesive

The adhesive provides the adhesion to the face sheet and core to transfer the load and also to work properly as a sandwich structure [9]. Suitable adhesive are available as a paste, liquid or dry film and include high strength and high modulus.

1.3 Core and Face sheets Materials

Glass fibers, Carbon fibers, Aramid fibers and Aluminum/Aluminum alloy are most widely used as a core as well as facing materials.

1.3.1 Glass Fibers

Glass fibers are made up of silicon dioxide and metallic oxide elements and are produced by drawing of molten glass through a small orifice as shown in figure 1.3 (a). E-glass (named for its electrical properties) and S-glass are the two types of glass fibers. Mostly E-glass is used as reinforcements in sandwich structures. S-glass has 30 percent higher tensile strength and 20 percent higher modulus than E-glass and is costly [14]. Glass fibers are mostly used in medium performance composites because of their high tensile strength that is maintained in humid conditions. Because of their relatively low stiffness, low endurance limit, and degradation when exposed to hygrothermal conditions they are avoided to use in high performance composites [8, 15]. Glass/epoxy and glass/polyester are extensively used in sandwich structures.

1.3.2 Carbon Fibers

Carbon fibers are mostly used advanced composite fibers and have a wide range of strength and stiffness depending on the manufacturing process. These fibers are manufactured from precursor organic fibers such as poly-acrylonitrile (PAN) or rayon. After heat treatments on these organic fibers, they are converted into carbon fibers as shown in figure 1.3 (b). To get graphite fibers high temperature pyrolysis (graphitization) is performed on the precursor fibers. As a result, carbon fibers are less than 95% carbon, whereas graphite fibers are at least 99% carbon.

Carbon fibers are mechanically and thermally anisotropic due to the nature of manufacturing process. In radial direction fibers have high thermal expansion and less stiffness as compared to axial direction. Graphite/epoxy and carbon/epoxy composites are now used extensively in sandwich structures [8, 16].

1.3.3 Aramid Fibers

Aramid fibers, are organic fibers extruded from the crystalline solution of sulfuric acid and polymer through small holes as shown in figure 1.3 (c). Aramid fibers provide high stiffness, low thermal conductivity that is good for heat resistance. Aramid fibers because of negative thermal expansion coefficient can be used in composite sandwich structures. Kevlar density is half of glass fibers, but its stiffness is higher than glass fibers. Kevlar 29 and 49 are known to be high and ultra-high modulus grades. Aramid fibers absorb moisture unlike other fibers that results in degradation of mechanical properties by 15-20% [16].

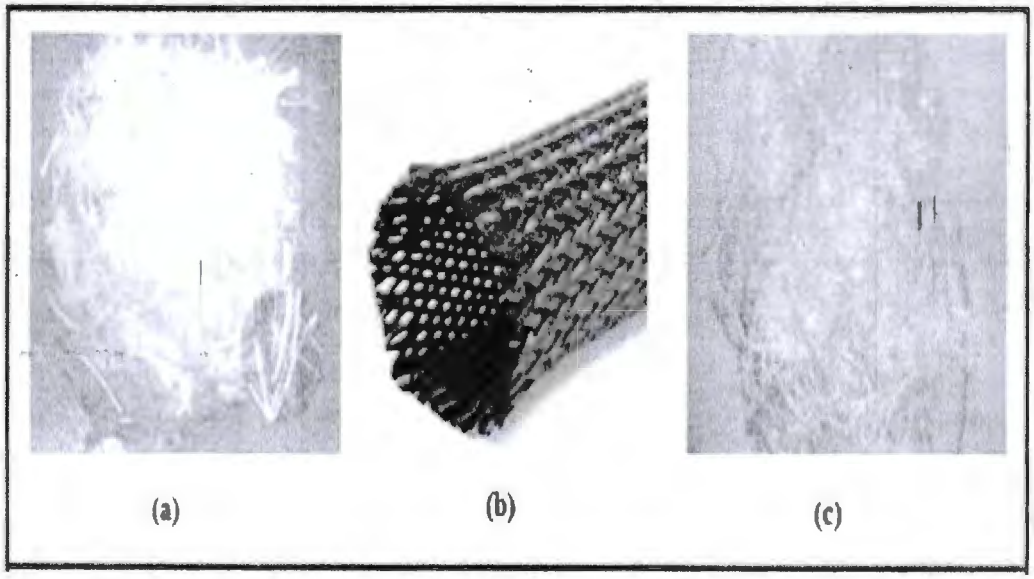

Figure 1.3: Reinforcement Types. (a) Glass Fiber (b) Carbon Fiber (c) Kevlar Fiber [8, 15, 16]

1.3.4 Aluminum and Aluminum alloy

Aluminum and aluminum alloy are most widely used because of light weight and less reactive with environment and high tensile and compressive strength. Aluminum 5052-H32, Aluminum 2024-T3, Aluminum 5251-H24, Aluminum 3104-H19, Aluminum 6061-T6 and others alloy are used as a facing material. [8, 16]

1.4 Classical Sandwich Structure Theory

After the world war two the description of behavior of sandwich structure began, In 1966 Plantema [17] presented the 1st book on composite sandwich structures. Zenkert [18] and Allen [11] follow the plantema and published the studies on the design parameters and failure behavior of sandwich panels. Gibson reported failure mode of sandwich structures [19] and developed a method for to design minimum weight sandwich structures [20].

The theory represented is referred as Classical sandwich structure theory. The basic assumption of this theory are:

1. Core carries entire shear load in composite sandwich structures.

2. The skins carry entire bending load.

3. Compression in core is negligible.

The Classical sandwich structure theory also assumes that the following discussed assumption are true by considering the skins and core elastic and by designing the structure in such a way that the length of panel must be high as compared to thickness, the thickness of face sheets must be very small as the thickness of panel and the skins to core mechanical properties ratio must be high.

Considering these assumptions the additional load carrying capacity of the core is negligible after its yield strength is reached [21]. However Mercado stated that the load carrying capacity of core continue to increase after yielding, this is because that the additional shear load is transferred to the face sheets. Due to this the load carrying capacity of structures increases 20-30 % of total load after the core yielding [21].

1.5 High Order Sandwich Beam Theory (HOSBT)

HOSBT was formulated by Frostig and Baruch [22], this theory relates the non-linear behavior of core during the bending of composite sandwich structure. The basic assumptions are:

1. Shear stresses present in core are uniform through the height of the core. Hexagonal Honeycomb configuration is shown in figure 1.4.

2. Vertical displacement of the core is a quadratic polynomial of z allowing the core to distort and its height to change.

3. Core is assumed as three dimensional elastic region, which has out of plane compressive and shear rigidity, whereas its resistance to in plane (1-2 plane) shear stresses is negligible.

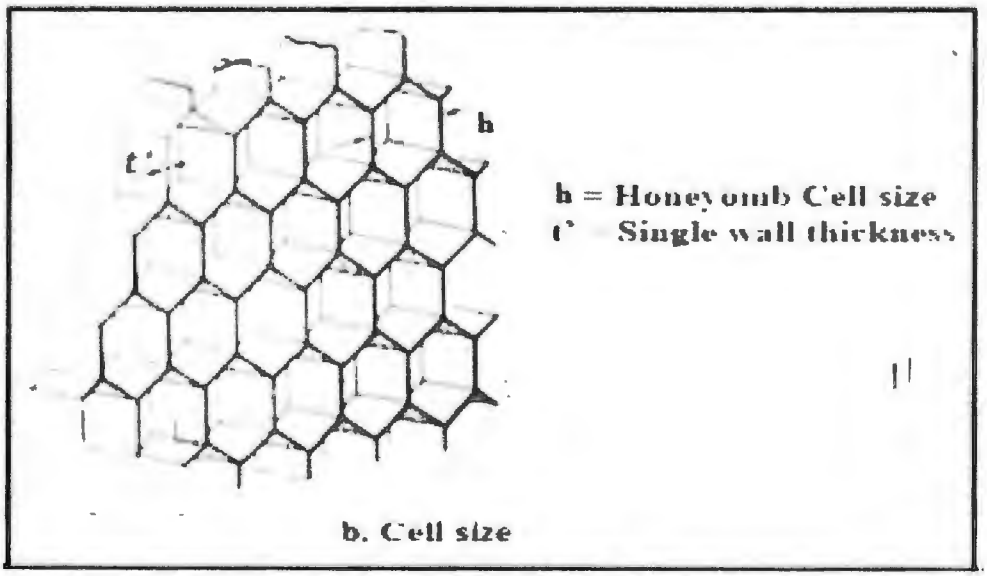

Figure 1.4: Hexagonal Honeycomb [22]

Petras et al [5] extended the HOSBT to examine the bending behavior and the localized effect of sandwich structure by formulating a sandwich beam with unit width and span L, which consists of core having thickness c, Shear modulus and Young's modulus G_c and E_c respectively and two face sheets having same thickness $t = t_t = t_b$, Poisson's ration and Young's modulus υ_f and E_f respectively as shown in figure 1.5 (b). The in plane displacements in the x-direction of centroid of the face-sheets are expressed as u_t and u_b, their corresponding vertical displacements as w_t and w_b respectively as shown in figure 1.5 (a).

Petras carried out the research to study the effect of point load instead of uniformly applied out and found that stresses in the upper face-sheet σ_{txx}, can be predicted as:

$$\sigma_{txx} \quad E_f\left(\frac{\partial ut}{\partial x}\right) \tag{1.1}$$

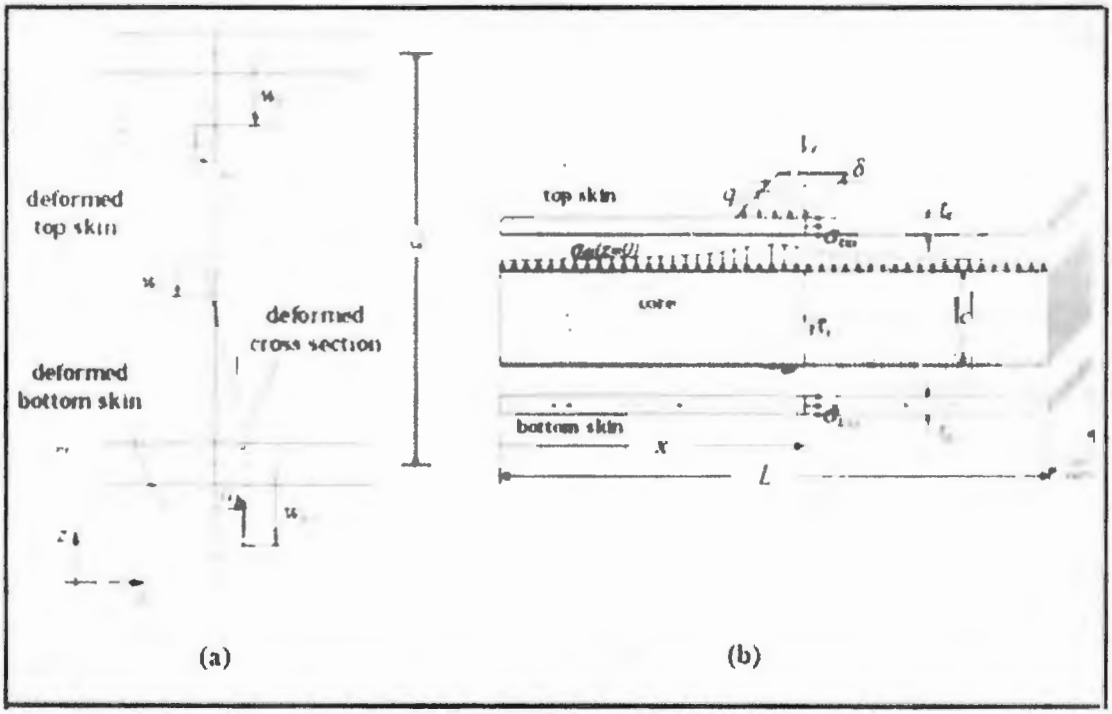

Figure 1.5: High Order Sandwich Beam Theory. (a) Non-linear Displacement (b) Beam geometry and stresses [5]

1.6 Failure Modes of Composite Sandwich Panels

Compression facing wrinkling, face yielding, core shear, local indentation and intra-cell buckling, bending of cell walls, delamination of face and core are the major failures observed in sandwich structures [23, 24]. The particular failure mode depends on the material properties of core and face, loading arrangement and the geometry of sandwich structure [5, 25]. The compression facing wrinkling is observed under three and four point bending. The indication of wrinkling is the sharp change in strain on compression facing. Wrinkling is short wave buckling of face sheet that is localized and is supported by an elastic continuum the core. Wrinkling is basically a local buckling behavior that occur in any form of web and causes the instability [6]. The core failure is observed under three point bending, core carries the shear load and in short beam test under three point bending the core fails when the maximum shear stress in the core reaches the critical value (shear strength) of the core. In long span beams the normal stresses in the core are of the same magnitude as shear stress, therefore the core is in biaxial state of stress and an appropriate failure criterion is needed to describe the failure of core. An indentation failure

is due to inadequate reinforcement or core is provided in the area under the load [25]. Most common failure modes under three point loading are shown in figure 1.6.

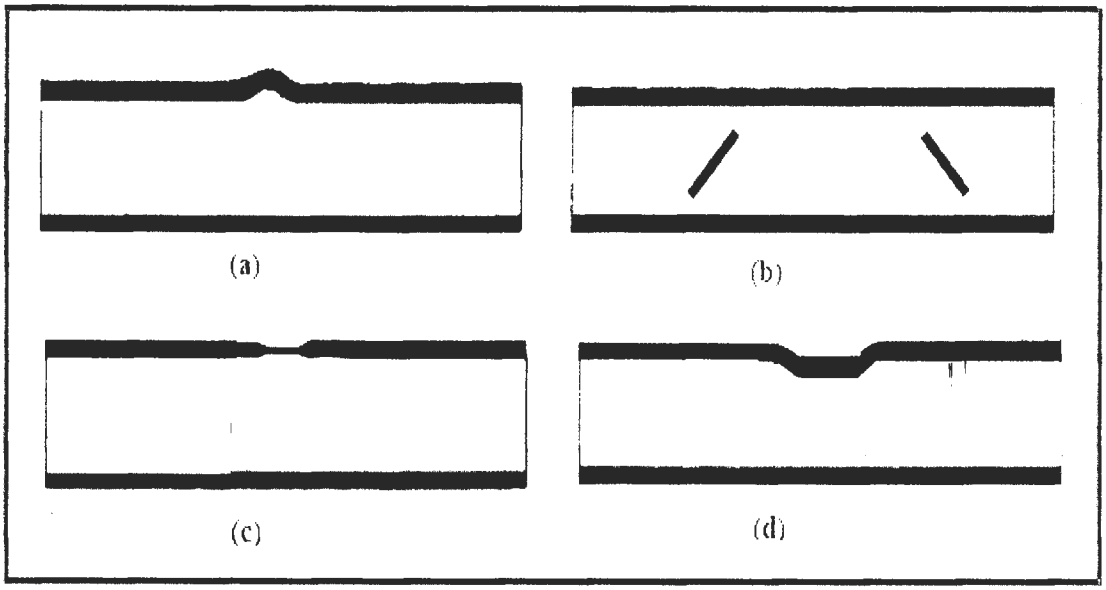

Figure 1.6: Failure modes. (a) Face wrinkling (b) Core shear failure (c) Face yield (d) Core indentation [26]

1.7 Research Problem

The mechanical behavior of composite sandwich panels has been widely analyzed because of the design problems considered in the fabrication and the particular use of these structures in several areas. The fatigue failure response of sandwich panels is also investigated [27]. But the performance of all types of honeycomb Sandwich Structures especially under fatigue loading, is still not completely understood because of large number of types of materials used for core and facing.

Glass fiber is slightly more flexible than carbon fiber also have lower tensile modulus which allows it bend and take more strain without breaking. Because of the Excellent corrosion resistance and low cost of fiber glass Aluminum honeycomb sandwich structure having face sheets of glass fiber not only used in same industries as sandwich structures having carbon fiber; it also have further applications. The Fatigue failure mechanism of Aluminum Honeycomb sandwich

structures having Glass fiber face sheets have not discussed. Therefore, this research is focused on sandwich structure having glass fiber face sheets and aluminum honeycomb.

1.8 Objective of Thesis

The aim of this research is to investigate the monotonic and the cyclic failure of composite sandwich structures having glass fiber face sheets and Aluminum skins. The secondary objective of this research is to investigate the real behavior of static and fatigue failure using both analytical and experimental analysis.

1.9 Research Methodology

The research has been carried out analytically and experimentally. The experimental approach has been carried out to investigate the flexural strength and stiffness of sandwich panels under static and fatigue failure loading. The camera and scanning electron microscope (SEM) is used to investigate the failure response after the loading of specimens.

The analytical portion is included to determine the strength of sandwich structures. The analytical analysis is also used to predict the expected failure mode. This figure 1.7 shows the flow chart of research methodology.

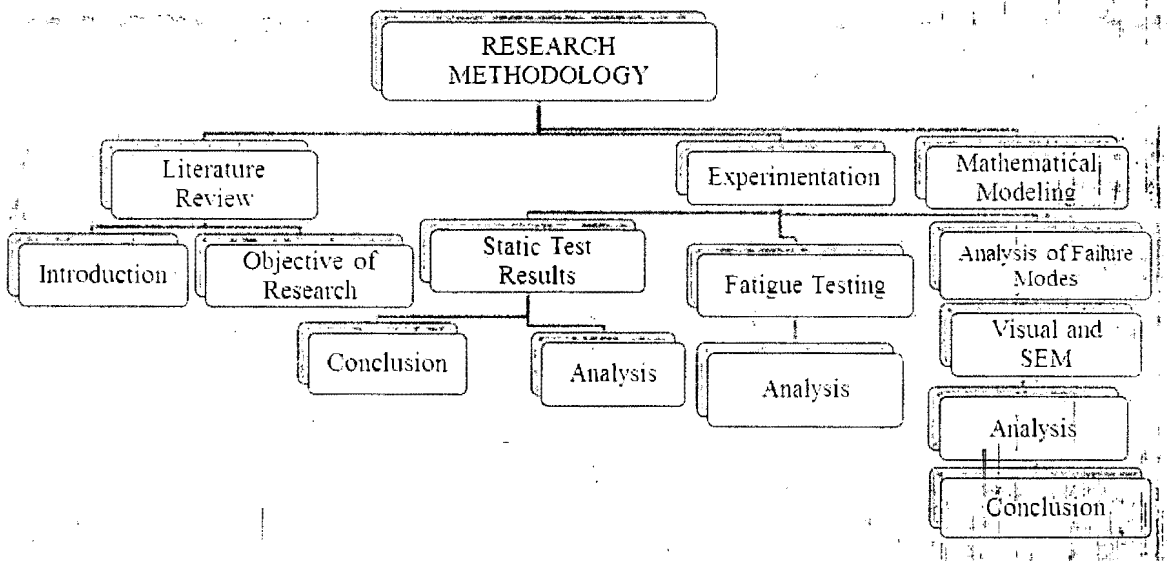

Figure 1.7: Flow chart of Research

1.10 Thesis Scope and Organization

In this thesis, several mechanical properties of the Aluminum/Glass fiber sandwich structures such as compressive strength, shear strength and bending strength, beam deflection and beam stiffness are investigated. The fatigue life of panel is also determine using stress and number of cycle behavior. The failure behavior is completely analyzed by using SEM. The following chapter is the introduction of sandwich structure. In this chapter constituents of sandwich structures, application, Failure behavior, objective and research methodology is briefly discussed. The next chapter is the literature review of the previous studies for static, fatigue and failure behavior of sandwich structures.

Chapter 3 describes the mathematical equations that are used to determine the flexural strength, fatigue life and expected failure mode. Chapter 4 describes the experimental setup for Static and fatigue loading and fracture mechanics studies. Chapter 5 presents the results and discussion of our experimental work and chapter 6 ends this dissertation the conclusions and future recommendations.

Chapter 2

LITERATURE REVIEW

This chapter covers the literature review of the static and fatigue failure response of composite sandwich panels. Following paragraphs describes the prominent studies on the sandwich structures.

Shan-shan Shi et al [28] performed three point bending test to determine the bending stiffness of composite sandwich structures of carbon fiber face sheets and aluminum honeycomb core with and without the Kevlar fiber Interfacial toughening. It has been observed that in the presence of Kevlar fiber the bending strength of sandwich structure improved. The static test result is shown in figure 2.1 (a). Crupi et al [29] compared the static and low velocity response of aluminum sandwich structures with foam and honeycomb core. The static test results are shown in figure 2.1 (b). It was investigated that the static response of sandwich structure changes with foam and honeycomb core as well as with the variation of the size of honeycomb core.

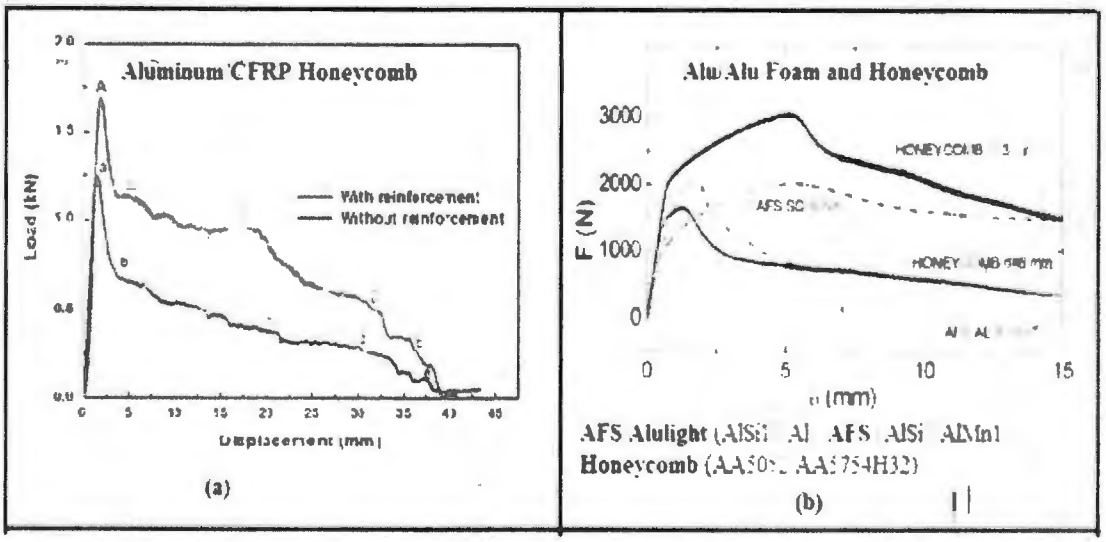

Figure 2.1: Load versus displacement behavior of honeycomb (a) [28], (b) [29]

Wahid Boukharouba et al [10] developed an analytical model verified by experimentation to describe the static and fatigue behavior of sandwich structure of carbon fiber skin and aramid core. It was investigated that the stiffness degradation during static and fatigue test is characterized

by three different phases as shown in figure 2.2 (a). Abbadi et al [30] have also performed four point bending test on two kinds of sandwich structures having aluminum 5754 faces and aluminum 3003 and aramid core one with defect and other without the defect. He investigated that the presence of defect have no effect on monotonic response of structure. And life time of structure is more in L direction than W direction. The static test result is shown in figure 2.2 (b).

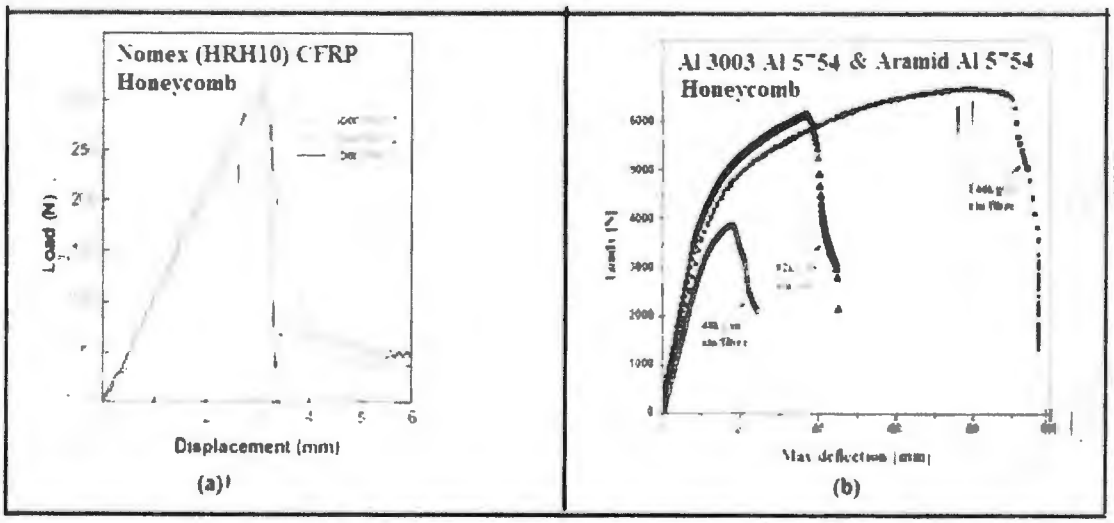

Figure 2.2: Load versus deflection behavior (a) [28], (b) [29]

Clark et al [31] studied the behavior of sandwich structures with Airex C70.30 core and glass/epoxy and aramid/epoxy fabrics face sheets under monotonic and fatigue loading. Fatigue tests were carried at a frequency of 1Hz. It was observed that the core shear failure increases at a higher rate near failure. A fatigue model was proposed for core dominated behavior based on fatigue deflection and fatigue modulus concept. It was observed that the rate of deflection increases rapidly near the failure as shown in figure 2.3. It was concluded that the core contributes very less in flexural stiffness therefore shear stress is assumed constant along the thickness.

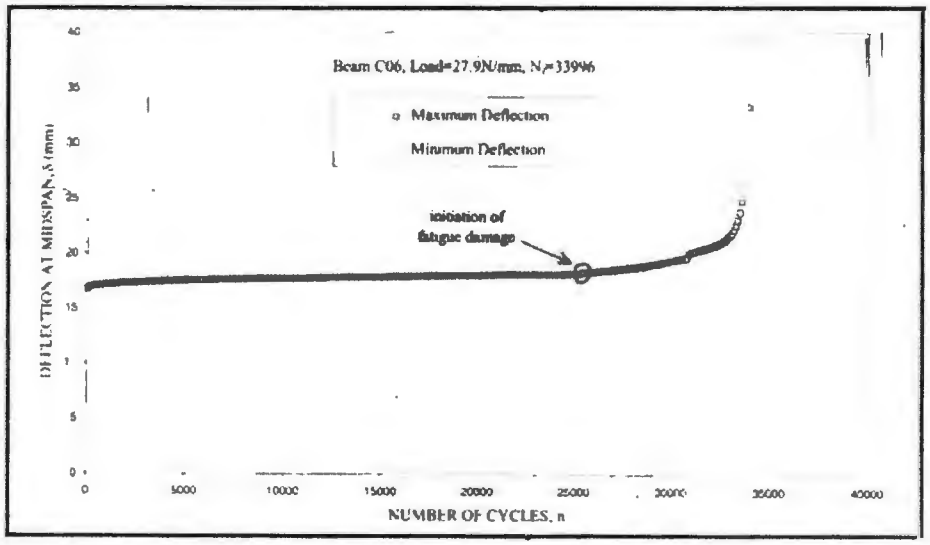

Figure 2.3: Fatigue deflection versus number of cycle response [31]

F. Cote et al., [32] performed three point bending test to access the static and fatigue strengths. An analytical model is also used to predict the static and fatigue strengths and failure modes. A good relationship is found between both analytical and experimental model. The relationship between deflection at mid span and number of cycle is shown in figure 2.4.

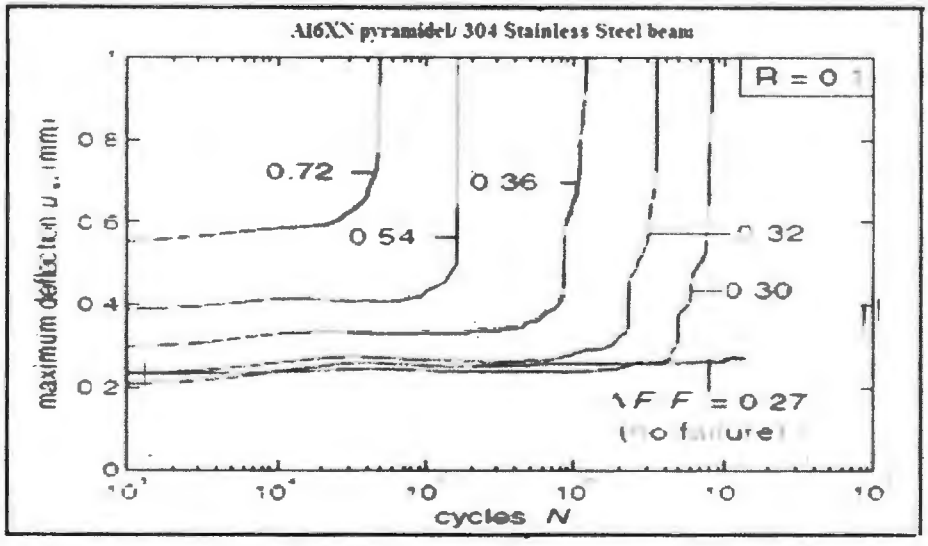

Figure 2.4: Fatigue deflection at different loading level [32]

Samirkumar M. Soni [33] investigated the fatigue failure behavior of composite sandwich structures with foam core and two types of face sheets E-glass epoxy and carbon glass epoxy using four point bending testing at room temperature (22°C) below to -60°C. It was observed that the fatigue failure at lower temperature starts immediately as compared to higher temperature. The stiffness degradation and initiation of failure is predicted by the relation between displacement at mid span and number of cycle as shown in figure 2.5 (a) and figure 2.5 (b).

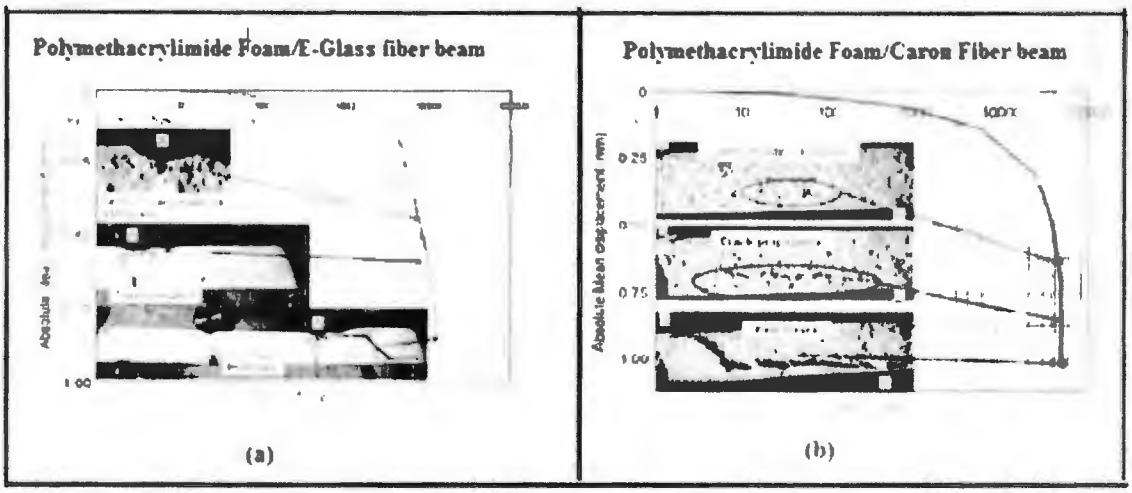

Figure 2.5: Deflection and number of cycle response [33]

Abbadi [34] proposed a fatigue model for core dominated behavior of composite honeycomb materials based on the degradation of stiffness for the four point bending test of sandwich structures for two different honeycomb configuration(L and W). The fatigue life of L configuration sandwich structures is more than W-direction sandwich structure at constant load level. The fatigue loading behavior is shown in figure 2.6.

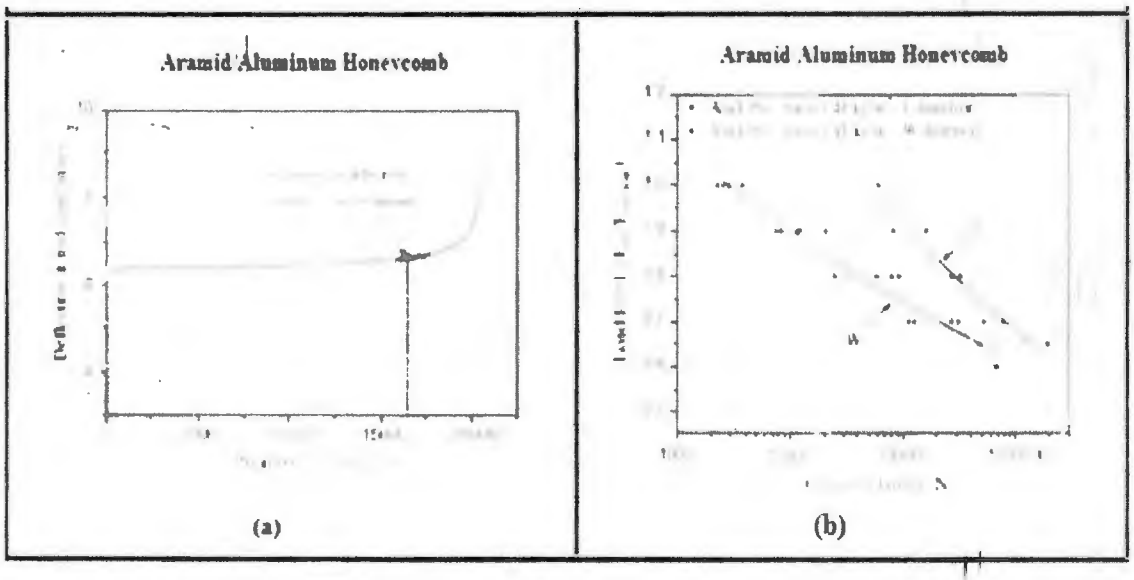

Figure 2.6: Fatigue loading response [34] (a) Deflection versus number of cycle response (b) Fatigue loading level versus no. of cycle response.

Burman et al [35, 36] studied the fatigue behavior of undamaged and damaged specimens of foam core sandwich beams. Fatigue tests on two sandwich configurations were used, one with Divinycell H100 (Poly-vinyl chloride, PVC) and other Rohacell WF51 (Poly-methacryl imide, PMI) core using the face sheets made of four layers of DBL 850 fabric/Vinyl ester 8084 and glass fiber/Epoxy respectively. The fatigue results were represented in standard S/N diagrams and curve to function is fitted using Weibull function as shown in figure 2.7. The load is represented in the ratio of fatigue load to static failure load and number of cycles are plotted as a logarithmic scale. The damage formation process including both initiation and growth in the test specimens was concluded that 90% of the fatigue life comprised of crack initiation and crack is initiated in the region of high shear stresses.

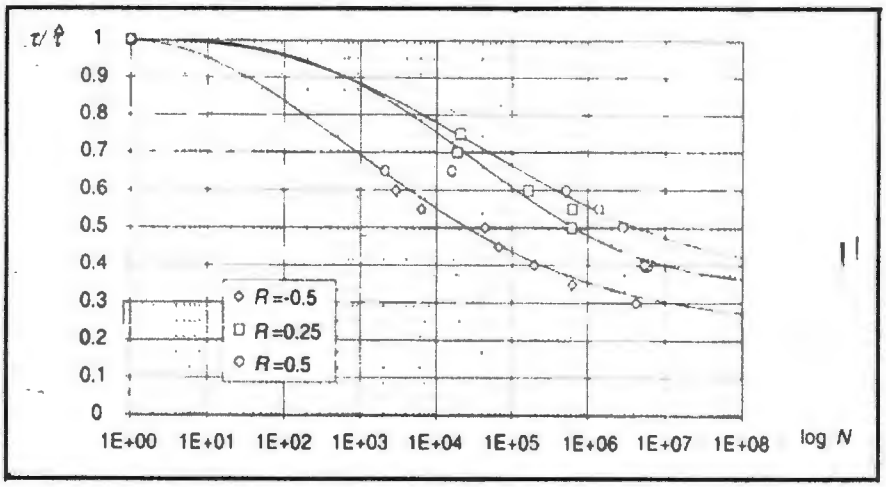

Figure 2.7: S/N curve for H100 [35]

Kanny et al [37] investigated the effect of fatigue loading on S2 glass fiber/ vinyl-ester with different PVC cores on the bases of different densities at a stress ratio of 0.1. In all the cases it was observed that increase in loading frequency result decrease in fatigue crack growth rate. The fatigue strength at different frequency is compared by the relationship between maximum stress and number of cycle behavior as shown in figure 2.8. Here H130 and R260 represents the 75 and 300 kg/m^3 of core. Also the fatigue strength increased with core density, and number of fatigue cycles to failure increased with increase in frequency.

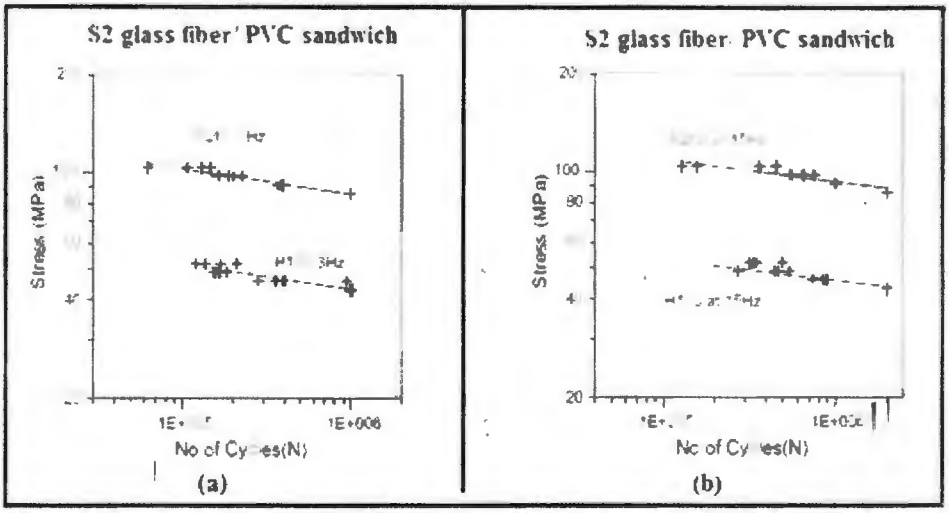

Figure 2.8: S/N data for beam for R260 and H130 [37] (a) at 3 Hz (b) at 15 H

Yi-Ming Jen et al [2] used the maximum bending stress and number of cycle behavior as shown in figure 2.9 (a) to investigate the fatigue strength of aluminum sandwich structure with aluminum 3104-H19 cores of various densities. Yi-Ming Jen et al [2] investigated the bending fatigue strength of sandwich structures on the bases of different amount of adhesive. It was proved that the fatigue strength increases with the amount of adhesive. The stress and number of cycle response is shown in figure 2.9 (b). In all of the cases it has been observed that with the decrease of applied stress the number of cycle to failure increases.

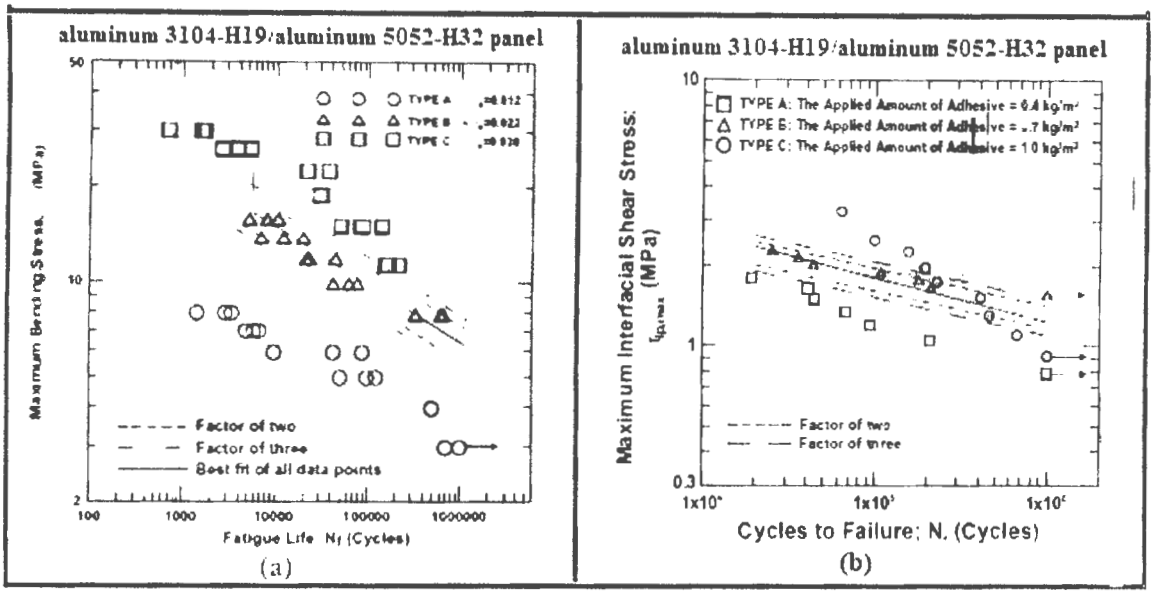

Figure 2.9: S/N data for beam [2] (a) cores of various densities (b) various amount of adhesive

Cunningham et al [38] proposed a technique for the estimation of core shear in closed sandwich structures of nomex honeycomb core and aluminum alloy 5070 B face sheets for three point bending static and dynamic loading. The strain was calculated by bonding the strain gauges on the face sheets and core on different locations, the calculated strains were then used to estimate the core shear strain. The limitation to the procedure is that it can be applied to only thin and equal face-sheets sandwich structures.

Gdoutos et al [25] carried out a thorough study on the failure mechanism of composite sandwich structure made up of carbon epoxy face-sheets and PVC foam core. The different studied failure mechanisms of sandwich structure were core failure, face-sheet indentation failure and face wrinkling subjected to three and four-point bending. In short span beam the dominating failure is

core shear failure while in long span beams the core is subjected to biaxial state of stress and an appropriate failure criterion is needed to describe its behavior.

L.L. Yan, B et al [39] compared the behavior of sandwich structure having foam filled corrugated cores with empty core sandwich structures using 3 point bending testing. It was proved that failure mode as well as flexural strength of panel changes with the amount of filling material (aluminum alloy). The failure modes during static test were shown in figure 2.10 (a). Face wrinkling, Face yielding, core shear and core indentation were observed during the different phases. It was observe that failure starts because of face wrinkling, but in our study in most cases the failure starts because of the core indentation this is because that the compressive strength of corrugated core is greater than honeycomb.

M. Dawood et al [40] investigated the static and fatigue response of GFRP sandwich structures with foam core. The experiments were performed to evaluate the density of fiber, thickness of structures and number of sheets in skin. It was predicted that the structures with flexible cores exhibited a lower degree of degradation as compared to stiffer cores. During static and fatigue loading initiation of failure starts because of the small shear crack in core. After the further application of load these cracks interconnected. The propagation of crack causes the interfacial de-bonding and rupture of fiber insertion. The failure behavior is shown in figure 2.10 (b).

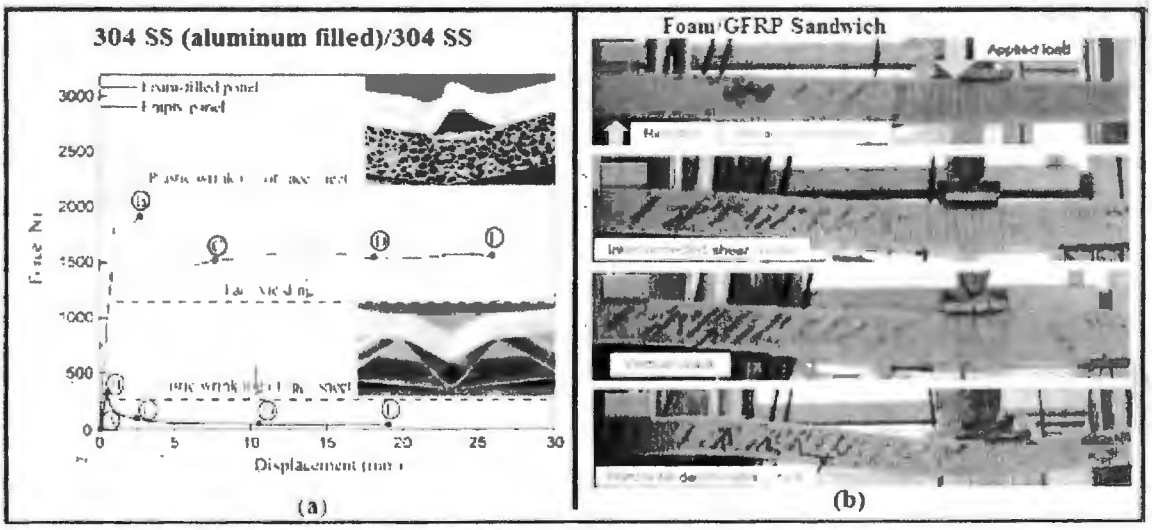

Figure 2.10: Failure modes (a) [39], (b) [40]

Belouettar et al [41] investigated the damage and failure modes of sandwich composites made up of aluminum honeycomb core and aramid fibers. The effect of core thickness and honeycomb cell configuration on the load carrying capacity and damage process was also investigated. The Flexural strength and fatigue life of panel is determined by the load and deflection and load and number of cycle response. It was observed that failure propagate in diagonal direction for L configuration and horizontally for W configuration. Also size of failure process zone is dependent on the loading span. For structural system aluminum core with L configuration are more suitable in operation. Face wrinkling, buckling of cell walls, fracture of cell walls and de-bonding of face sheets and honeycomb interface are observed that are given in figure 2.11.

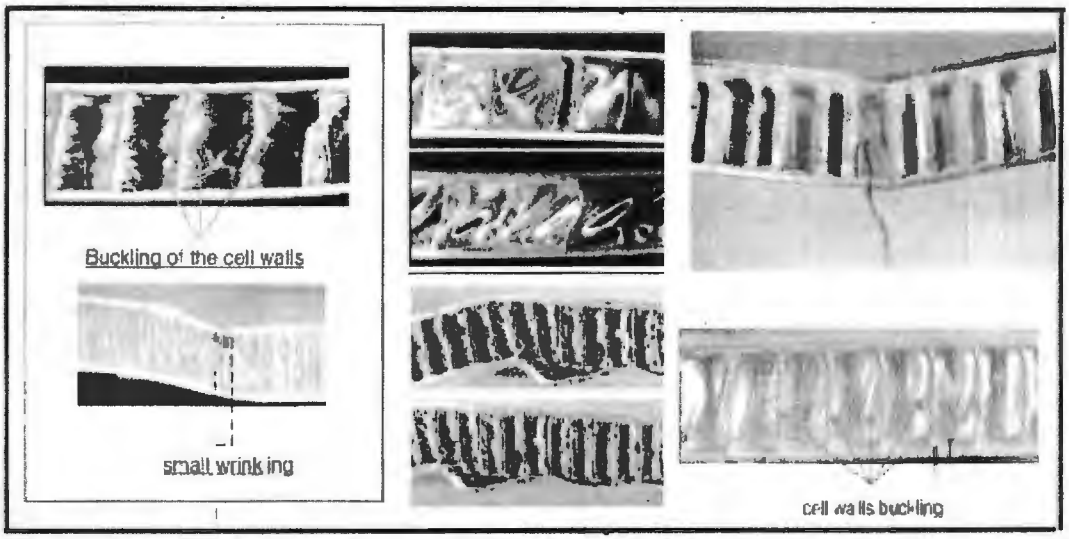

Figure 2.11: Failure modes of aluminum honeycomb in L direction [41]

Kulkarni et al [27] investigated the fatigue crack growth in flexural loaded foam core sandwich beams, estimated the fatigue life based on crack propagation rate and developed a fatigue model based on crack growth. The de-bonding of face-sheet and core was observed to be the first failure in sandwich structure comprising 15% of specimen life. This de-bond propagates slowly along the top face-sheet/ core interface (up to 60% of fatigue life), then kinked in to the core (up to 85% of fatigue life) and finally into the lower face-sheet/core interface and then propagated abruptly. Fatigue life model for both high cycle and low cycle fatigue were developed that were in good agreement to the experimental result.

T. McCormack et al [26] predicted that the sandwich structure failed by different failure modes that are face wrinkling, face yielding, core yield and indentation. The observed failure modes are given in figure 2.12 (a). F. Cote et al., [32] used SEM to access fatigue failure behavior. It was found that the fatigue failure initiated at the interface between the skin and brazed joint as shown in figure 2.12 (b).

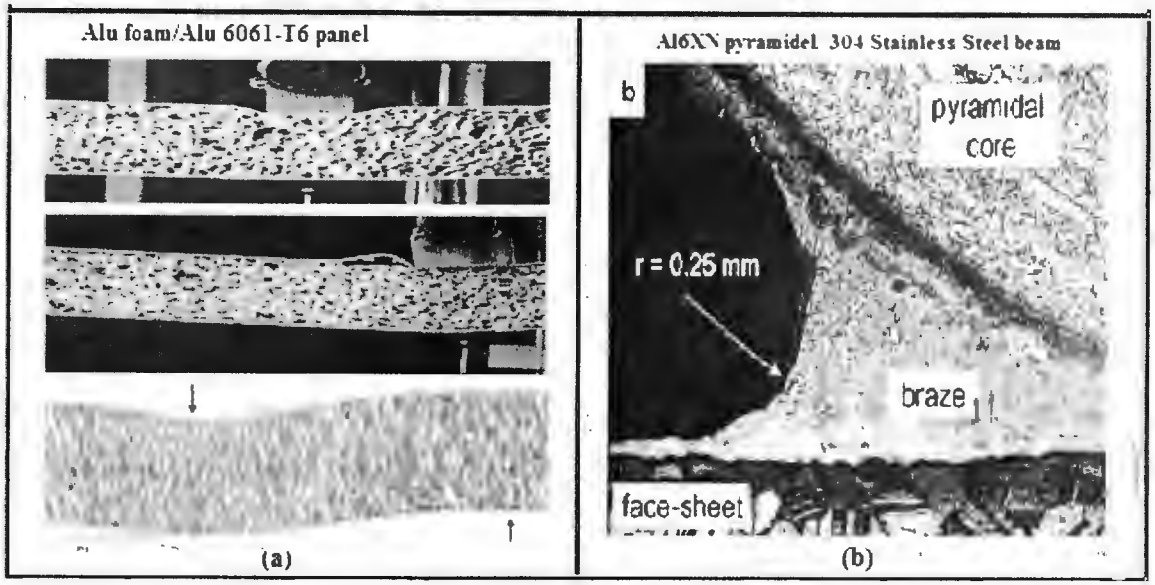

Figure 2.12: Failure mechanism [26] (a) Failure observation during loading (a) Failure observation using SEM

Pan Shi-Dong et al [42] investigated the longitudinal shear deformation behavior of aluminum alloy 5056 honeycomb and categorized the core shear deformation into four stages named as plastic deformation, elastic deformation, fracture of cell wall and de-bonding of face-sheets/ honeycomb core interface. The modified shear buckling theory neglecting the effect of adhesive produced more reasonable and acceptable results that are 56% less accurate than experimental results. Belingardi, Martella and Peroni [43] experimentally investigated the fatigue response of initially un-damaged and damaged sandwich structures subjected to four point bending. The compressive failure in upper face-sheet was observed in un-damaged specimens while in damaged specimens the structure failed due to core shear at the tip of de-bonded portion. The fracture in honeycomb was at the upper portion of cell wall where tensile stresses are maximum and then propagated through the thickness of core.

Styles et al [44] studied the effect of core thickness in aluminum foam core sandwich structure with thermoplastic composite facing and concluded that decreasing core thickness increases the chances of skin wrinkling, core cracking and crushing failure. The thick specimens on the other hand failed due to core indentation, the core indentation was eliminated using high thickness face-sheet but it promotes the core shear cracking.

Jen et al [45] studied the effect of face-sheet thickness on the fatigue strength of the three types of sandwich structures with aluminum honeycomb. The experimental results for the same applied load showed no apparent relationship between face-sheet thickness and fatigue life of specimens. The main failure was de-bonding at the interface of core and face-sheet. Local interfacial stresses were evaluated using finite element simulation. Three parameters peeling stress, interfacial stress and linear relation of the two were observed, it was concluded that linear relationship of peeling stress and interfacial stress gave more accurate results then the individual parameters.

Banghai et al [1] developed an theoretical model to predict the failure modes in case of three point bending testing. Three point bending test was also carried out to verify the analytical approach. It was found that the initial failure modes may be face yield, core shear are core indentation.

Zenkert et al [46] designed and studied the behavior of sandwich structures subjected to fatigue loading. They concluded the sandwich structures subjected to lower loads and greater number of fatigue cycles fails due to core shear whereas structures subjected to high loads and small number of fatigue cycles generally fails by face tensile failure. For the quasi static fatigue loading the sandwich structure may fail under face tensile fracture because the slopes of core shear failure and face tensile failure are different.

Manalo et al [47] studied the flexural behavior of sandwich structures made up of glass fiber reinforced polymer skins and phenolic core. The strength of sandwich structure in flatwise and edgewise positions was determined and it was showed that composite sandwich positioned edgewise fail at higher loads with less deflection as compared to the specimens tested in flatwise position. It was also observed that composite sandwich under flexural loading failed due to

progressive failure of skin when positioned edgewise and brittle core shear failure br compressive skin failure along with de-bonding was observed for flatwise positioned specimens.

Gibson et al [48] extended the laminated beam theory to the sandwich structure along with fracture mechanics to analyze the core shear failure and the cracks that initiate as a result of core failure in foam core sandwich structures. The model is formulated only for crack initiation and it don't work for crack propagation and kinking that was observed in experiments on carbon/epoxy face sheets or E-glass/epoxy face-sheets with polymethaacrylimide foam core. It was observed that the crack initiate near the face-sheet core interface for glass fiber face-sheets and in the middle of the core for carbon fiber face-sheets. This is because carbon fibers are five times stiffer than glass fiber.

Rao et al [49] studied the fatigue and flexural behavior of E glass/ vinyl-ester with polyurethane foam sandwich structure at different test frequencies of 1Hz, 3Hz, 5Hz, 8Hz, and 9Hz and revealed that the strength of structure is dependent on the cyclic load and test frequency, change in core density effects the foam-face sheet de-bonding failure.

Herranen et al [50] carried out the strength calculations for different materials in order to find a new solution to the design of light weight sandwich panel for trailers. The sandwich structures were fabricated using vacuum infusion technology and subjected to four-point bending. Ansys is used for simulation purpose. It was found that design is more sensitive to core material selection than core thickness and use of core materials like polymethaacrylimide doesn't provide significant improvement in mechanical properties rather leads to sudden increase in cost.

Zhenkun et al [51] proposed an improved six step phase shifting photo-elasticity method for the sandwich structures to analyze the shear stress field in the core of sandwich structure in addition to load transfer and local stress concentration. The load transfer is observed by the color bands between upper and lower face-sheets. It was observed that the core shear stress is distributed evenly in four-point bending, but distributed anti-symmetrically in three point bending.

Chapter 3

ANALYTICAL MODELING

In order to use composite sandwich structures in different areas, the better understanding of their static and cyclic behavior is required [10, 34]. For an optimum design weight or stiffness/unit weight must be minimum. Lorna Gibson & Mike Ashby [52] describe the complete analysis in "Cellular Solids - Structure and Properties". The analysis is same for different types of bending loads except different forms of geometrical constants.

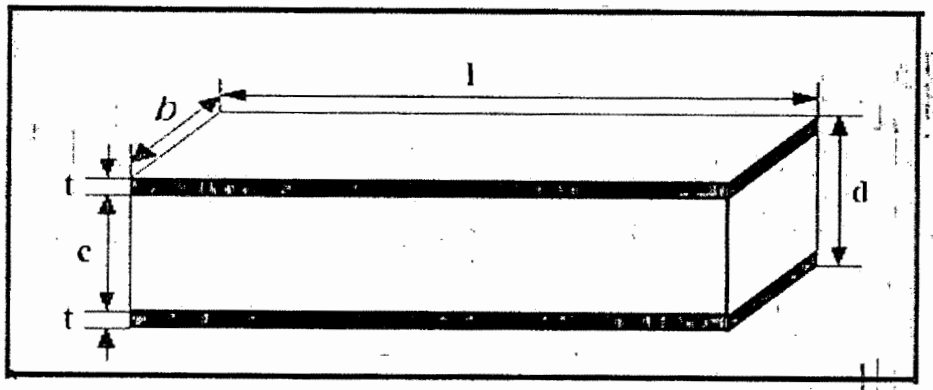

Figure 3.1: Sandwich panel measurements

The figure 3.1 show the design measurements of sandwich panels, where l is the span length, b is the width, c is the thickness of core , and t is the thickness of face sheets. The d is the thickness of beam (d = c+2t).

3.1 Calculation of Normal and Shear Stresses in Face sheets and Core

To understand the specific failures it is necessary to develop the distributions of stresses in faces and cores as shown in figure 3.2. During the loading both normal and shear stresses acts on the panel. These stresses depends on the bending moment and the distance from the mid line of panel.

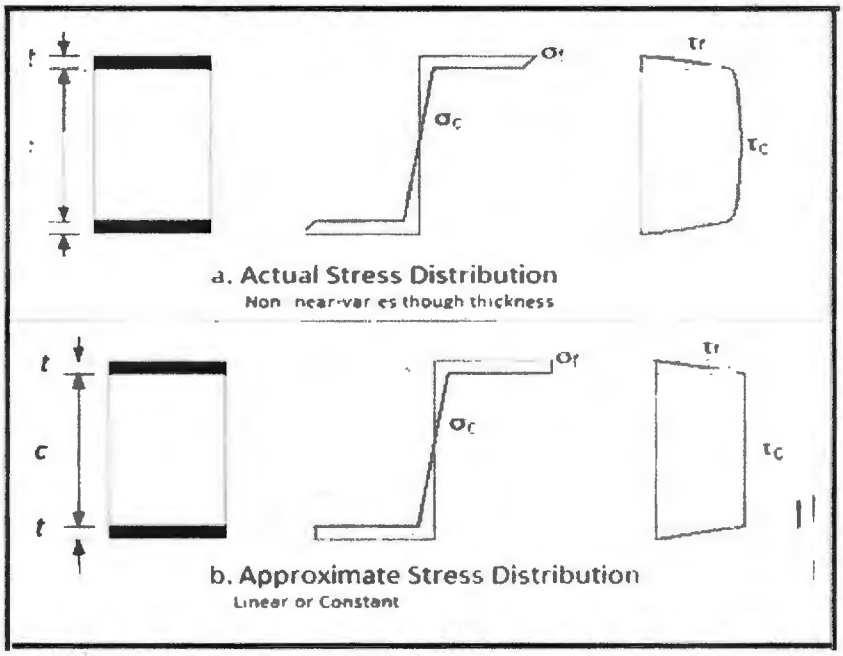

Figure 3.2: Stress Distributions. (a) Actual Stress Distribution (b) Approximate Stress Distribution [52]

Given that σ_f and σ_c for the normal or compressive stresses in the face sheets and core and τ_f, τ_c for the shear stresses. ρ_c, ρ_f are the densities of core and faces and E_c, E_f are the modulus of elasticity of core and facing skins.

$$\sigma_f = \frac{M_y E_f}{BS} = \frac{M}{btc} = \frac{Pl}{Abtc} \tag{3.1}$$

$$\sigma_c = \frac{M_y E_c}{SS} = \frac{ME_c}{btcE_f} = \frac{PlE_c}{btcE_f} \tag{3.2}$$

Where M is the bending moment, P is applied load, BS and SS are the bending stiffness of the panel. A is constant depends upon the type of loading. Where E_c may be determined by

$$E_c = CE_f\left(\frac{\rho_c}{\rho_f}\right)^2 \tag{3.3}$$

$$G_c = DE_f\left(\frac{\rho_c}{\rho_f}\right)^2 \tag{3.4}$$

Where C (~1) and D (~0.4) are constants and G_c is the shear modulus of core in the direction of load.

Shear stresses are calculated by:

$$\tau_c = \frac{P}{Bbc} \quad (3.5)$$

$$\tau_f = \frac{t_c}{2} \quad (3.6)$$

Where B is also a constant and its value depends upon the type of loading. For 3-Point Central Loading configuration the values of A and B are 4 and 2 respectively.

3.2 Calculations of Maximum Bending Strength

The maximum Bending stress of sandwich structure [2] is calculated by

$$\sigma_b = \frac{M\left[\frac{c}{2}+t\right]}{I_t} \quad (3.7)$$

Where bending moment is M, and calculated by taking the product of Maximum Applied Load (F_{max}) and half span length (l/2). M may be calculated by using the equation: $\sigma_f = \frac{M}{btc}.I_t$ is the transformed moment of Inertia along the horizontal axes and calculated by:

$$I_t = 2\left[\frac{bt^3}{12} + bt\left(\frac{c}{2}+\frac{t}{2}\right)^2\right] + \frac{1}{12}bc^3 \quad (3.8)$$

3.3 Beam Stiffness and total Deflections

The strength of beam in bending is estimated from the equivalent flexural rigidity or bending stiffness (BS) of beam, and the equivalent shear rigidity or shear stiffness (SS) of beam [52].

$$BS = \frac{(E_f btc^2)}{2} \quad (3.9)$$

$$SS = \frac{(G_c bd^2)}{c} \quad (3.10)$$

$$\text{As } c \approx d \qquad SS = G_c bc \quad (3.11)$$

The deflection [52] is considered as the sum of the shear and bending components, when load is applied.

$$\delta = \delta_b + \delta_s = \frac{PL^3}{24E_f btc^2} + \frac{PL}{4bcG_c} \quad (3.12)$$

3.4 Prediction of Modes of Failures

With the information of distribution of stresses on cores and faces and different parameters depending upon the types of loading we may predict the mode of failure after loading. [19]

3.4.1 Face Yielding

When the tensile stress is equal to strength of facing material then mode of failure is Face Yielding.

$$P \geq \sigma_f \frac{Abtc}{l} \quad (3.13)$$

3.4.2 Face Wrinkling

When the normal stress in the compression skin of the panel reaches the level of instability then the face wrinkling occurs.

$$P \geq \frac{Abtc}{l} 0.57[E_f E_s^2 \left(\frac{\rho_c}{\rho_s}\right)^4]^{\frac{1}{3}} \quad (3.14)$$

3.4.3 Core Shear Failure

The shear stresses in the core are greater than the normal stresses so when the maximum shear stress increases from the shear yield strength of the core, core Failure may occurs. This shear yield strength depends upon the density of core material.

$$P \geq CAbc \left(\frac{\rho_c}{\rho_s}\right)^{\frac{3}{2}} \sigma_s \quad (3.15)$$

3.4.4 Bond Failure

If the strain energy release rate increases the critical rate of strain energy for the adhesive, then bond failure will propagate, Using M=Pl/B3 the failure load is then

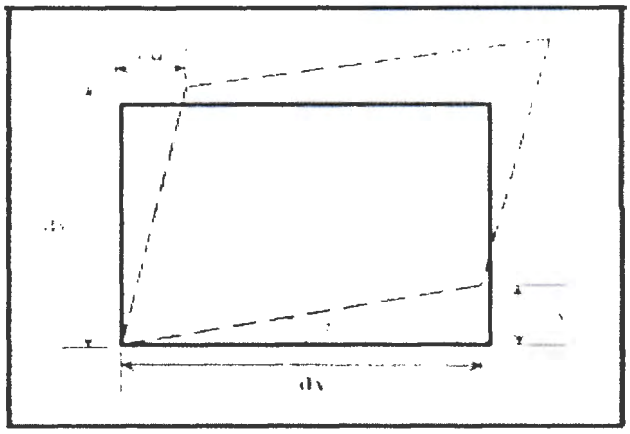

Figure 3.3: Shear strain [4]

For the element shown in figure 3.3 the angle α is positive in the anti-clockwise direction and β is positive in clockwise direction, now if the element only rotates then the sum of the two angles will give zero. But in the case of non-zero shear the sum of the two angles will not be zero. Shear strain can be calculated as:

$$\tan\alpha = \frac{\partial v}{dx} \quad ; \quad \tan\beta = \frac{\partial u}{dy}$$

$$\alpha = \tan^{-1}\left(\frac{\partial v}{dx}\right) \quad ; \quad \beta = \tan^{-1}\left(\frac{\partial u}{dy}\right)$$

$$Shear\ Strain = \frac{\left|\left(\frac{\partial v}{dx}\right) + \left(\frac{\partial u}{dy}\right)\right|}{2} \tag{3.19}$$

According to the fundamental bending theory of sandwich structures, when the sandwich element deforms due to an applied load the resulting deflection is the sum of primary or bending and secondary or shear deflection. The bending deflection is because of bending of sandwich structure about its neutral axis, and shear deflection is due to the produced shear strain in the low transverse modulus of rigidity core [4]

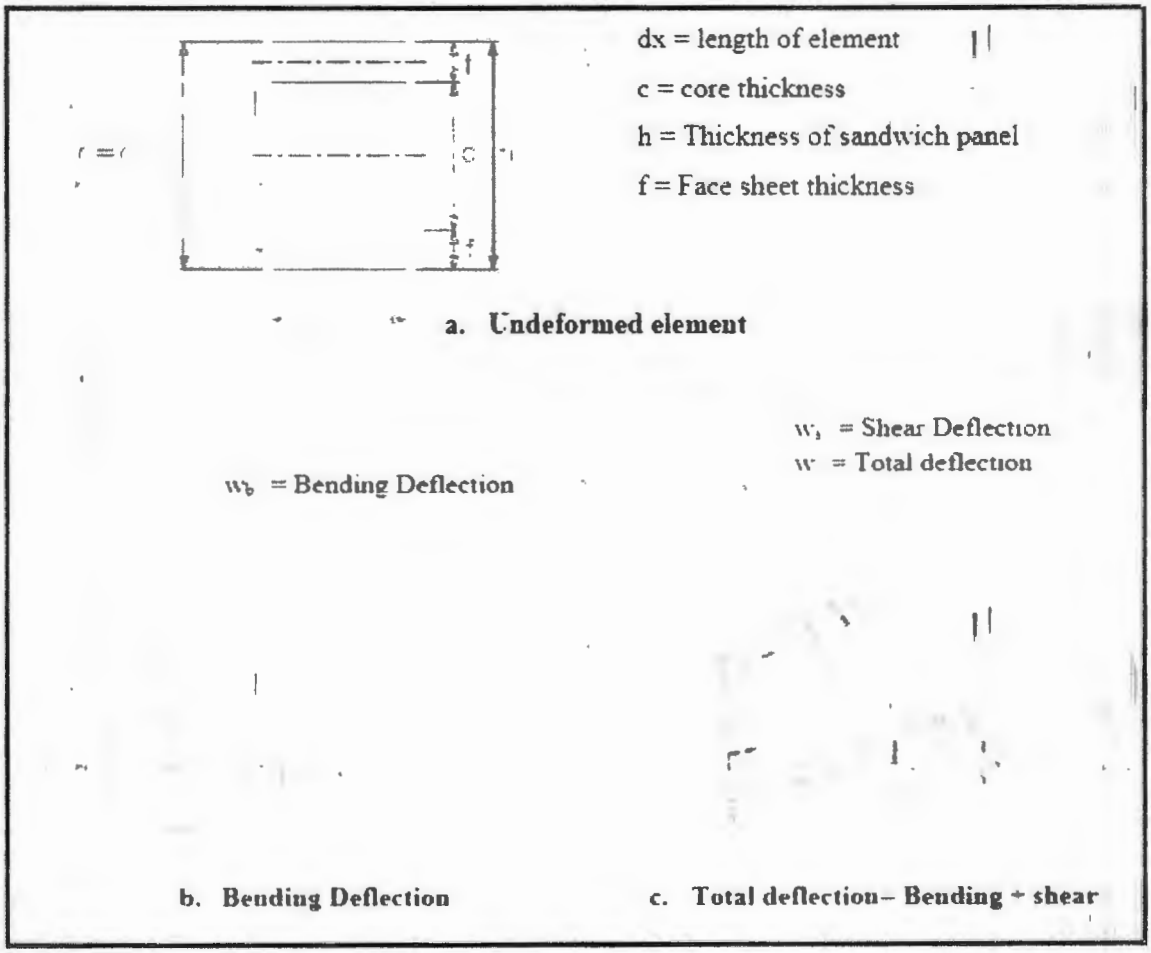

Figure 3.4: Sandwich Element Deformation [4] (a) Undeformed element, (b) Bending Deflection, (c) Total deflection

During the bending the sandwich elements undergoes partially bending deflection and partially shear deflection. To account only the effect of shear strain we have to eliminate the effect of bending deflection from the calculations. Let we assume only half of the element as shown in figure 3.4, the X and Y are the axis of the un-deformed element, X'Y' representing the rotated element and X''Y'' representing the deformed element. The deformed element X''Y'' has rotated by an angle O and at the same time getting shear equals to the sum of shear angles $\gamma 1$ and $\gamma 2$.

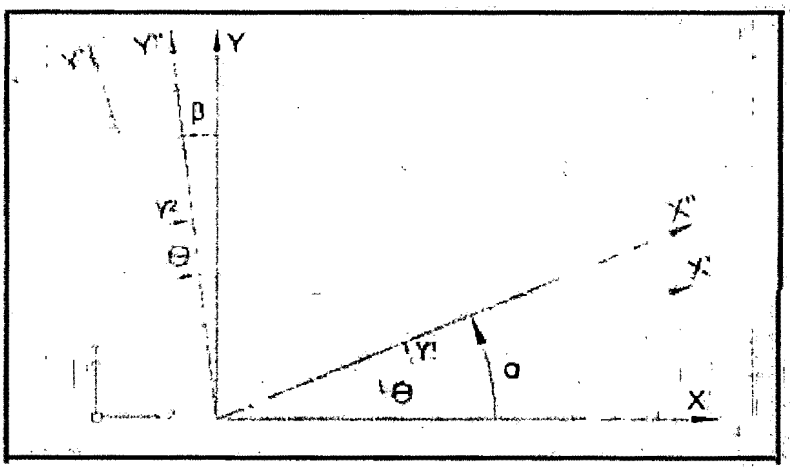

Figure 3.5: Sandwich element deformation under bending loads [4]

The angle α is positive in counter-clockwise direction and β in clockwise direction. For the specified case when will we add up α and β according to equation 3 the shear strain is given as:

$$\text{Shear strain} = (\alpha + \beta)/2 = [(\Theta + \gamma 1) - (\Theta - \gamma 2)]/2 = (\gamma 1 + \gamma 2)/2 \qquad (3.20)$$

To find the shear strain we assumed an element passing through center of four subsets. When the bending load is applied on the sandwich structure due to rotation and shear the coordinates of the element will be changed. The new coordinates of deformed image can be compared with the un-deformed image to measure the shear strain according to the equation.

3.5.1 Linear Strain measurement

Linear strains are produced in the upper face-sheet and lower face-sheet as a result of bending of sandwich structures. It is generally assumed that all the bending loads are carried by face-sheet and upper face-sheet will undergoes compression while lower face-sheet undergoes tension. But the stresses in the upper and lower face-sheets are the combination of tensile and compressive stresses. The stresses in the face-sheet become critical so that they cause failure of the sandwich structure because of face wrinkling; face sheet indentation, debonding etc. The linear strain is found by measuring the length of each element in reference image and then comparing it to the deformed image as:

Linear Strain = (Deformed Length – initial Length)/initial Length

For the calculation of linear strain of an element in the upper face-sheet, if the length of the element is a in un-deformed or reference image and after deformation its length becomes b then linear strain can be calculated using equation as:

Linear Strain $[(b - a)]/2$ (3.21)

Where 'a' is the length of the un-deformed element and deformed element 'b' is found using the distance formula between two consecutive points.

The accumulative linear strain in the upper face-sheet is calculated for all the images and then plotted against time to get an idea of the damage in the face-sheets with applied fatigue cycles. Similarly the linear strains are measured in the lower face-sheet. In addition to it a comparison of linear strain in the upper and lower face-sheets is also made to observe the dominating failure mode in the sandwich structure.

3.5.2 Calculation of absorbed Shear Strain Energy

During the fatigue loading of sandwich structure the specimen doesn't come back to its initial state. In fact, it absorbs some amount of energy in each cycle, and the resistance of the sandwich structure to the shear strain decreases. This effect can be calculated by measuring the area under the curve of force vs. shear strain graph. Trapezoidal rule can be used to estimate the area under the curve by integrating the function f(x) from the interval 'a' to 'b'.

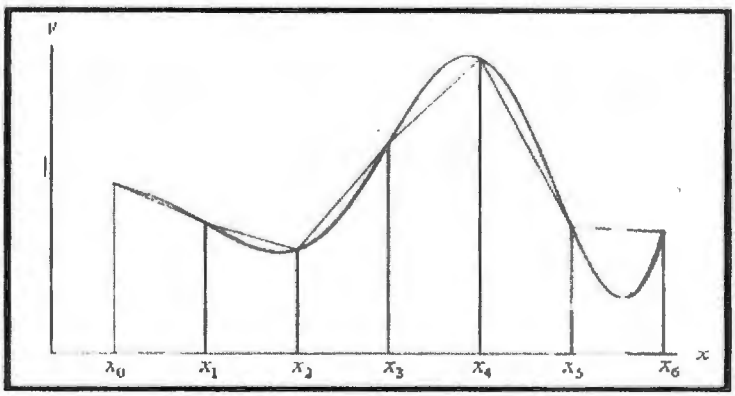

Figure 3.6: Integration of function using Trapezoidal Rule [38]

$$\int_a^b f(x)\,dx \approx \frac{\Delta x}{2}\,[f(X_0) + 2f(X_1) + 2f(X_2) + \ldots\ldots\ldots\ldots + 2f(X_{n-1}) + 2f(X_n)] \quad (3.22)$$

Increment = (upper limit – lower limit)/ no. of increments

$$\Delta x = (b - a) / n \tag{3.23}$$

The area under the curve calculated using trapezoidal rule will give us the energy absorbed by the sandwich structure during bending. The energy at each cycle divided by the energy of the first cycle gives a non-dimensional absorbed shear energy criterion. The need to non-dimensional energy is because the total energy under the force-displacement hysteresis curve is the sum of normal strain energy and shear strain energy which has units of joules. The energy calculated from shear strain hysteresis curves is not in joules. To compare the relationship between the total energy and shear strain absorbed energy we adopted non- dimensional energy criterion. A non-dimensional shear absorption energy law is formulated for 1 and 3 plies sandwich structures with W configuration and then extended to sandwich structure containing 5 plies with L orientation. The decrease in energy absorption (indication of damage) is governed by the power law.

$$\Phi_{i,j} = \Lambda N^{\beta} \tag{3.24}$$

Where

Φ = Absorbed Shear Energy

i= No. of face-sheets

j = core Configuration

N= No. of cycles

β = Scaling exponent

Λ = constant

It compares the evolution of absorption of energy due to shear during cycling for materials with different face-sheet thicknesses and gives an idea that how the energy absorbed during the flexural fatigue loading of sandwich structures is effected by the thickness of the face-sheet and the orientation of the aluminum honeycomb in the core.

Chapter 4

EXPERIMENTAL PROGRAM

To understand the static and fatigue failure behavior of the composite sandwich structures different types of experiments can be performed. In this research work different types of experiments are performed that are Static (for monotonic loading) and Fatigue (for cyclic loading) and failure behavior is analyzed using different techniques.

This chapter provides the specific information about all the tests, test specimens, test procedure, and techniques.

4.1 Standard Test Method

ASTM standards C 393 and C 394 [53] are used for the determination of sandwich shear stiffness, facing strength, core shear strength, flexural stiffness and core shear fatigue. 3-point (Mid Span) loading configuration was established as a standard loading condition to attain the mode of failure as shown in figure 4.1. Multiple Loading configuration e.g. 4-point loading configuration, Quarter point loading configuration are considered as non-standard. But In industry it is difficult to compare the data obtained from these condition with standard test method [54] because the strength of sandwich structures changes with the change of loading configurations. Following points [55] must be considered for the selection of Test specimen.

i. According to the ASTM standard C 393 the specimen should be in rectangular shape.
ii. The depth of the Sandwich Structure must be equal to the beam thickness.
iii. The breadth of the specimen should be twice of its total thickness, equal to or more than the three times the size of core cell.
iv. The standard span length must be 150mm.
v. The length of the specimen must be equal to the span length of three point bending apparatus plus 50mm (2in) or plus one half the sandwich thickness.

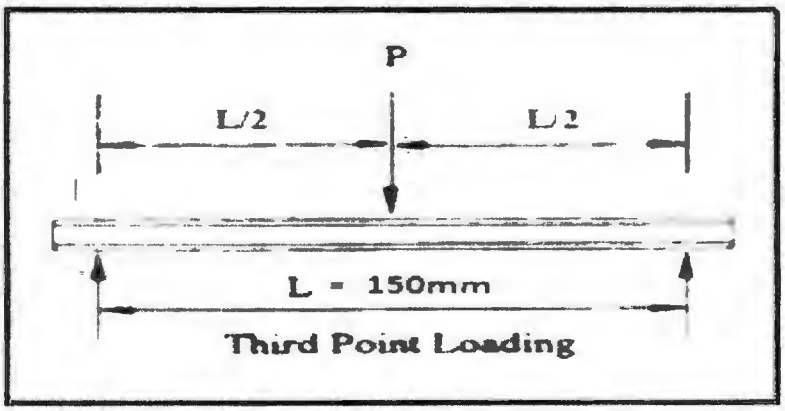

Figure 4.1: ASTM C-393 Three point loading configuration

4.2 Specimen

The composite sandwich structure used in the specimens is of Hexcel aluminum honeycomb [56]. The Detail of material is as under.

4.2.1 Material

Face-sheet is made up of woven glass fabric as reinforcement and epoxy as matrix. The epoxy used contains Araldite and Aradur that are mixed properly to obtain the optimal properties. The glass fabric provides the high strength to weight ratio. Woven Glass fabric is characterized by high strength, low coefficient of thermal expansion and good chemical and biological and fire resistance.

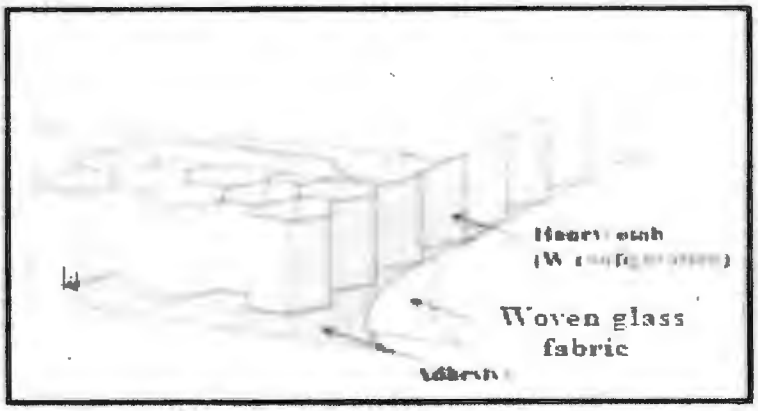

Figure 4.2: Sandwich structures panel with honeycomb configuration

Honeycomb Core is made of Aluminum 5052-H32. The two principal directions of honeycomb are Ribbon (L direction) and the other one is the transverse direction (W direction) as shown in figure 4.2 and 4.3. The properties of the honeycomb structure vary in these directions; normally the strength of the honeycomb in the L direction is twice than that of W direction.

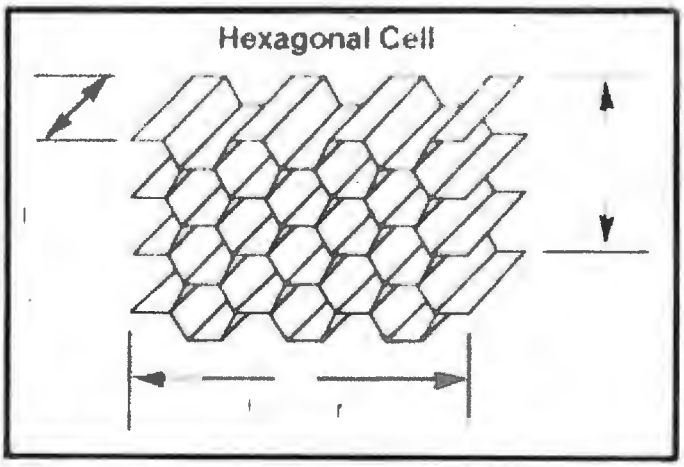

Figure 4.3: Honeycomb cell configuration

Mechanical properties of core and face sheet are given in table 4.1. Aluminum Honeycomb panel used for static and fatigue testing is shown in figure 4.4.

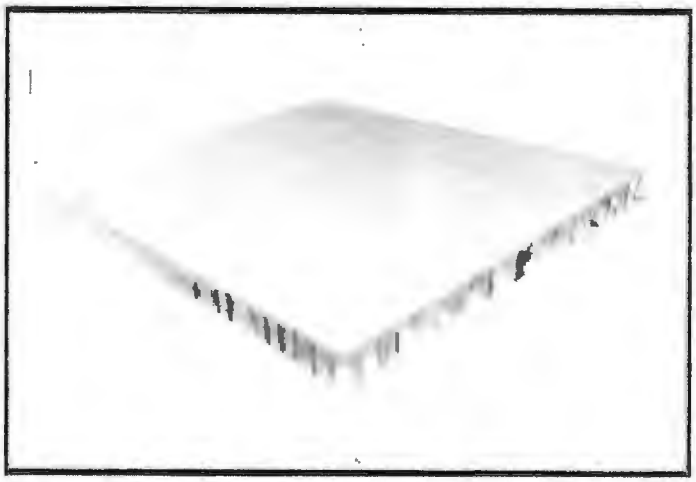

Figure 4.4: Aluminum honeycomb panel

Table 4.1: Mechanical Properties of Aluminum Honeycomb Core and Face sheet

Properties	Core wall Aluminum 5052-H32	Face sheet E-glass fiber
Density	83 kg/m^3	0. 47 kg/m^2
Poisson's ratio	0.33	0.125
Elongation (%)	13	4.8
Tensile Modulus (GPa)	70.3	20
Compressive Modulus (GPa)	1.31	17

4.2.2 Dimensions

The three-point bending static and fatigue testing is proposed to carry insight of the dominating failure modes of the sandwich structure following ASTM C393. For this purpose a total of six sandwich composite structures are tested. After cutting according to the ASTM standard we have the specimen as shown below in figure 4.5.

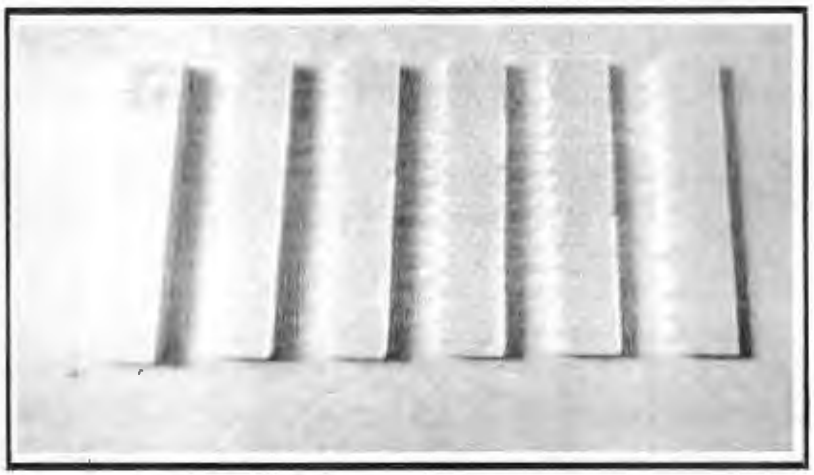

Figure 4.5: Aluminum Honeycomb specimens

The geometry and dimensions are shown in figure 4.6.

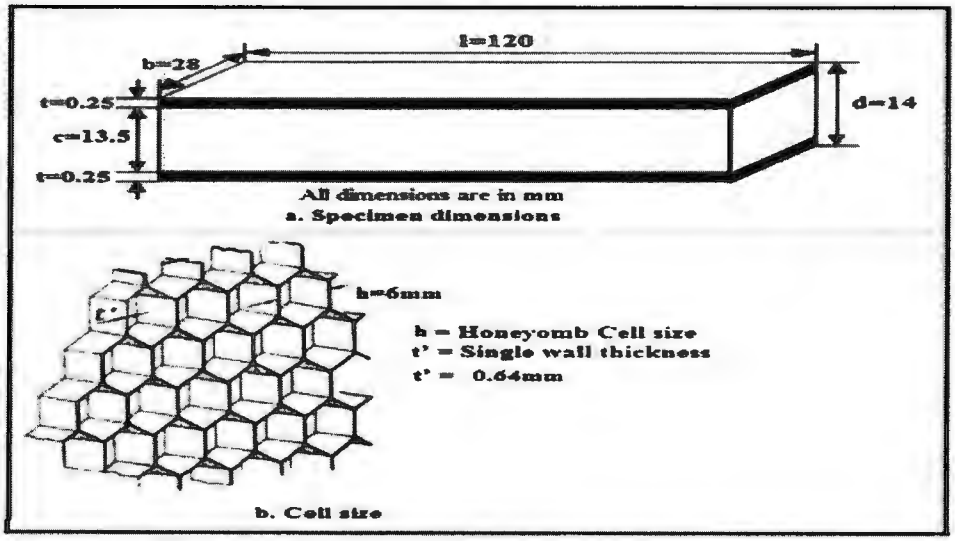

Figure 4.6: Specimen Parameters

4.3 Experimental Method

Two types of experimental setup were used for the initiation and propagation of failure through static and fatigue loading and fracture mechanics studies to understand the failure behavior of structure.

4.3.1 Static and Fatigue Testing

Both monotonic and dynamic tests were carried out through a 3-point bending testing fixture using the Material Testing System (MTS-810). MTS as shown in figure 4.7 is an indispensable resource to obtain the information about the characterization of all types of materials and available in Fracture Mechanics lab of UET Taxila. Force range from 25KN to 500 KN. The ability to test materials ranging in strength from plastic to aluminum, composites and steel. The span length of the bending test fixture used in tests (shown in figure 4.7) was adjustable to accommodate different size of specimens.

Its Static Hydraulic system is used for compression, shear, tension and flex/bend testing. Accurate Fatigue tests were performed using the same load unit cell for monotonic tests. The system's controller (Flex test material testing system) is used to show the results in hysteresis as

well as in numeric in arranged form. A camera connected with laptop is used to show the loading and unloading on the specimen during the testing.

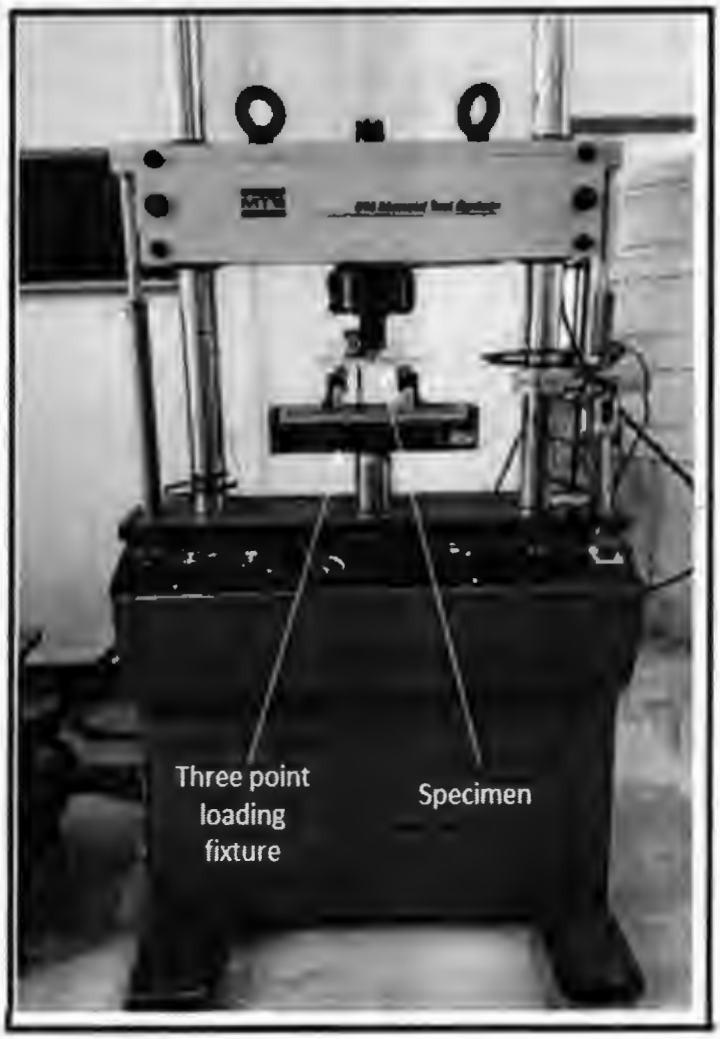

Figure 4.7: MTS-810

The 3-point bending monotonic tests were carried out using the load cell of 100N at the rate of 2 mm/min at constant displacement amplitude as shown in figure 4.8. The load increases rapidly until a material fails. The evolution of force and displacement was observed on computer screen. Also the deflection along the span length was recorded with the increase of force.

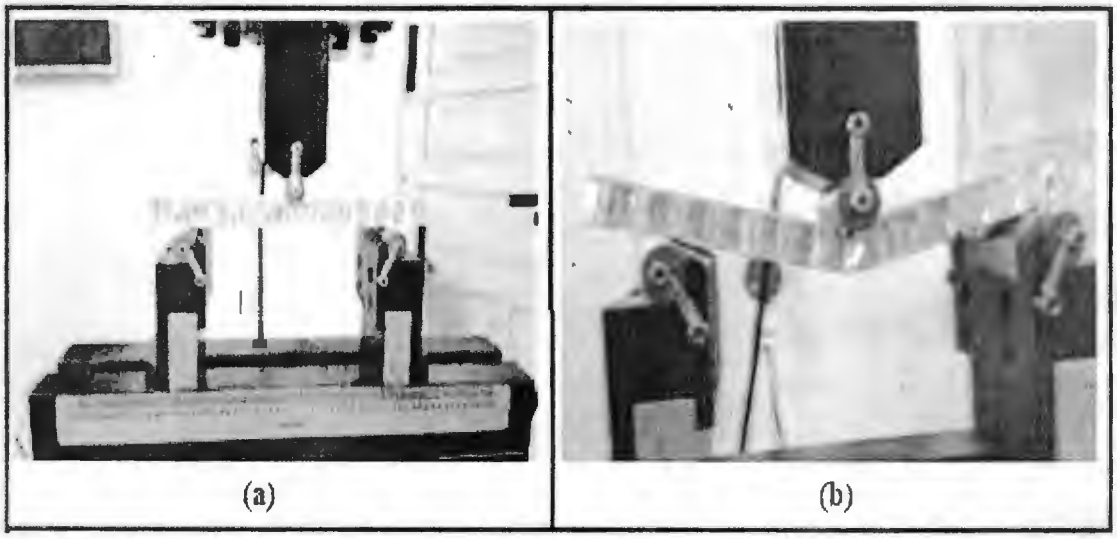

Figure 4.8: Specimen during testing. (a) Under loading (b) After failure

Cyclic loading was performed using the same unit load and fixture configuration at constant amplitude loading as shown in figure 4.9. The data of loading were obtained from the static load by taking the load ratio 0.1. The operating frequency was 2 Hz. The target set point and amplitude of loading was calculated by considering the loading and unloading in periodic oscillations of constant amplitude by a sine function. So sine curve was selected for constant amplitude loading. The data of force and deflection was recorded after the completion of preset a number of cycles by decreasing the frequency near about zero. The movement of unit load was observed by the camera. The increase in deflection was considered as the initiation of failure that was also analyzed by camera. It was noted that in start the displacement of specimen along the mid span remained same after the thousands number of cycles but this deflection increases which shows the stiffness degradation of specimen.

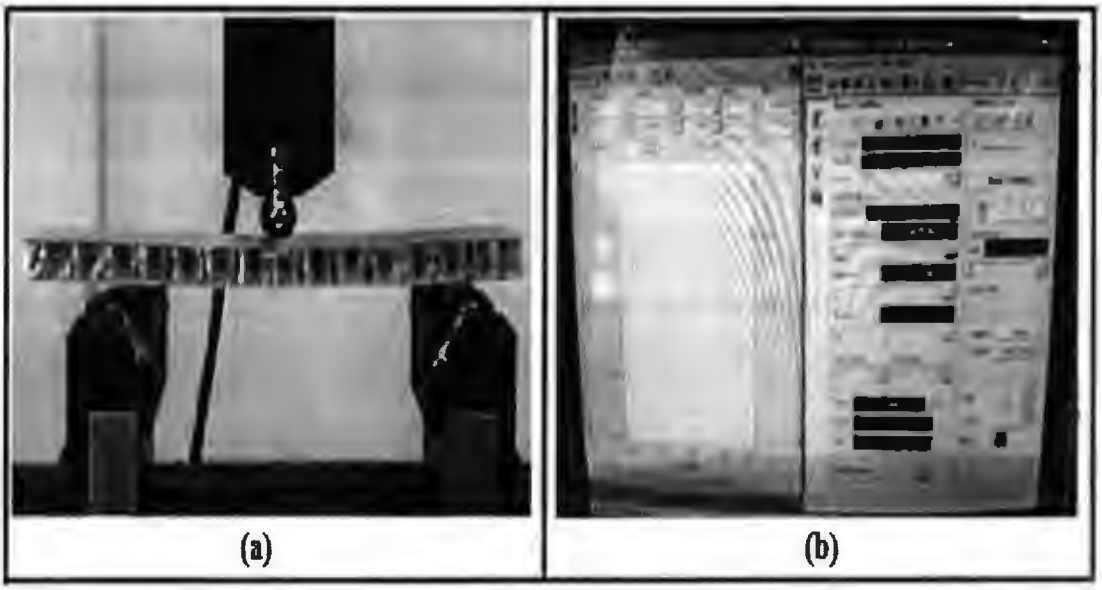

Figure 4.9: Specimen under loading (a) After fatigue failure (b) Controller

Friction free actuators and stiffness of load unit to ensure the best possible resolution and test control, making this material testing system suitable for both static and fatigue testing application. Following test procedure is given below.

i. Define the test

Calculated the test parameters and define the system configuration before proceeding with the test procedure. These calculations and configurations include the following:

- Defined the type of test.
- Selected the test control mode.
- Defined the test program.
- Selected the program source.
- Calculated the forces and/or displacements to be achieved during the test.
- Calculated the span and setpoint control settings.
- Determine the types of fixtures/grips needed to secure the specimen into the load frame.

ii. Set up test components.

Set up the load frame, data acquisition devices, and test controller as defined in step. The setup tasks include the following:

- Prepared the fixtures/grips, specimen, and data acquisition transducers.

• Ensured that the load cell is properly rated for the test and that it is aligned with the actuator.

• Ensured that the servovalve and feedback control cables are properly connected.

• Verify that the test controller is correctly configured for the test and for the desired signal monitoring.

• Set up the data recording/acquisition devices.

iii. Turn electrical power on.

Electrical power to a console-mounted controller is typically controlled by the main **Power O/I** switch located on the console lower front panel. Desktop of floor standing controllers typically have the **Power O/I** switch located on the back panel of the unit.

iv. Set transducer full-scale values.

The transducer full-scale values associated with the calibrated range are set up in Station Manager after station Builder has configured the transducer (sensor).

v. Complete initial servo loop adjustments.

To set the servo loop controls to levels that will ensure actuator stability, complete the following steps. Ensured the actuator stability at hydraulic startup, selection of low proportional gain and stabilization settings is recommended for first-time operation or setup. When using the system for similar tests on similar specimens, this step can be eliminated after the servo loop has been properly adjusted for one test.

4.3.2 Failure Modes Studies

To determine the failure behavior of sandwich panels Scanning Electron Microscope (SEM) have been used. For this purpose only a defective portion of a composite sandwich structure have been separated from specimen as shown in figure 4.10. SEM is used for the microscopic surface study of conductive materials. By using scanning electron microscope used focused beam of high energy electrons to generate a variety of signals at the surface of specimens. Data is collected over a selected area of the surface of the sample. Area of specimens under examination was 1 cm in width was imaged in a scanning mode, magnification ranging from 20X to approximately 30,0000X, spatial resulation of 50 nm to 100 nm.

Figure 4.10: Specimen for SEM

Because of non-conductivity of fiber glass first of all face sheets of fiber was coated by ultra-thin layer (2-20nm) of conducting metal Gold (Au) using Sputter Coater as shown in figure 4.11. This is the standard method for poorly conducting or non-conducting specimens prior to observation in a SEM.

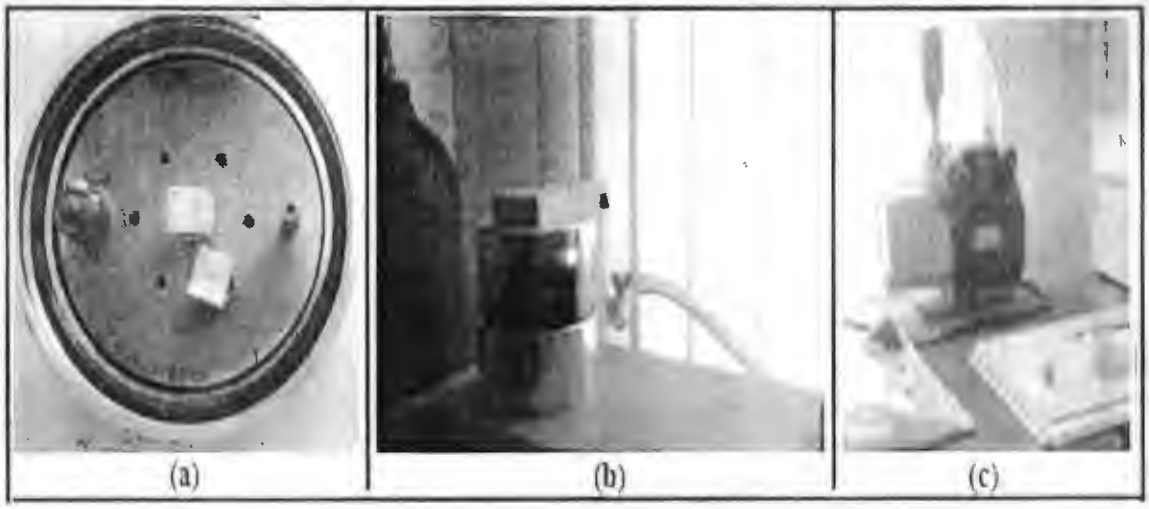

Figure 4.11: Sputter coating setup. (a) Specimens (b) Chamber (c) Motor

After the gold coating specimen were placed for the failure studies with a SEM as shown in figure 4.12.

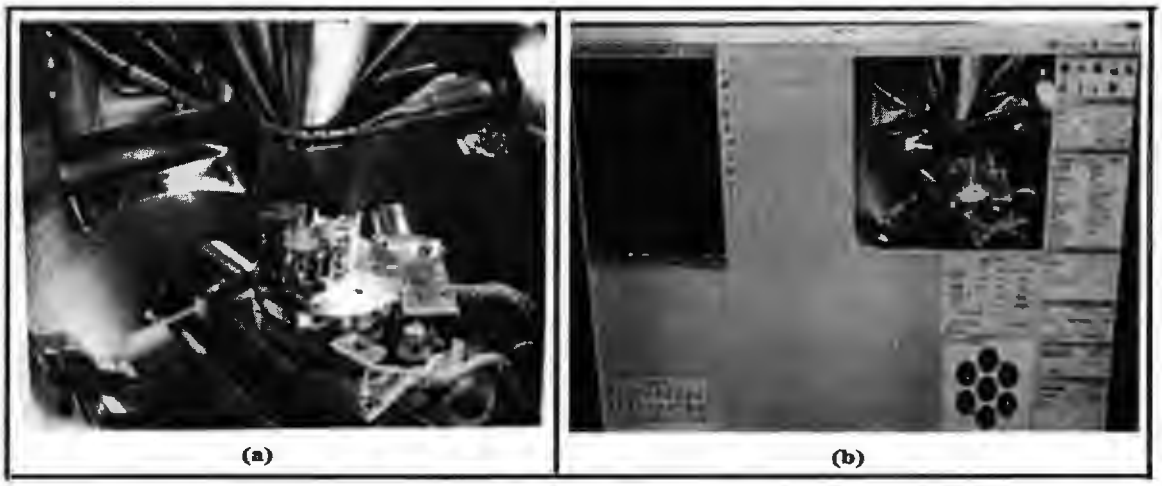

Figure 4.12: Scanning Electron Microscope Setup (a) Specimen (b) Controller

The three portions of specimen upper fiber glass face sheet, aluminum honeycomb core and fiberglass interface and an aluminum honeycomb core from the side have been analyzed. First of all complete portions of one of the above was focused and then defective portion was magnified and images of this portion were saved using the controlled computer. Such as first of all the images of coated face sheets having view field of 916 μm was taken at the magnification of 151x. After this image is magnified more and more to observe the only damage portion and the images were recorded. Such as image of 160 μm face sheet was analyzed at the magnification of 868x. In such a way all of the sides were completely examined to find the any possible defect. The procedure of testing is given below.

i. Sample preparation
ii. Sample coating
iii. Sample holding
iv. Sample grounding: samples are electrically connected to the sample holder and placed in chamber
v. SEM login using the user account.
vi. SEM image screen: The set of 6 tabs on the right side of the screen contain command and parameter setting buttons for setting the SEM up for imaging.
vii. Sample loading: The sample is prepared and mounted on the SEM sample mount, we have to vent the SEM to load it. This is done by clicking on the Sample Exchange icon in the

upper left of the SEM image screen. After the sample is properly mounted onto the SEM stage and inspected, gently closed the chamber door. Just as it closes, it will "latch" closed by the force of a magnet at the back of the stage so that the door will be held closed against the sealing O-ring when the vacuum pump starts, thus preventing an old problem of sucking room air into the chamber because the o-ring is not well sealed. Now click OK in the box on the screen asking "Press OK to Pump." The pump down sequence will take several minutes to achieve sufficient vacuum in the chamber for the system to open the column valve and establish a beam. In the meantime, you can click on the "Vacuum" tab in the right hand panel of the screen to view the vacuum level in the chamber and the gun. The gun should be below 8x10-10 Torr and the chamber vacuum line will be grayed out until the vacuum achieves a measurable level. The chamber will eventually achieve something in the low 10^{-6} Torr range.

viii. Establishing the Electron Beam: As the vacuum level in chamber drops below $7.5x10^{-5}$ Torr, the column valve was opened and the gun EHT (High Voltage) will "Run Up." By clicking on the Gun tab on the right side of the SEM screen, we observed the gun conditions.

ix. Stage Control: When the a beam is established, the substrate needs to be positioned under the column so the beam can see it. This requires moving the stage from its default loading position to the inspection location which may depend on the sample and its size and shape. Before moving the stage, bring up the "Chamber Scope" window by clicking on the "Eye" icon at the lower left task bar of the right side LCD monitor. This will bring up a window into the SEM chamber viewed from the rear looking toward the front door. The image is an optical image illuminated by 6 LEDs.

x. Check Sample Current Monitor Status: In order to insure that the Sample Current Monitor is off, activate the SCM window by clicking on the thin blue border of the SEM image screen to expand a menu having the SCM selection; double click on the SCM listing and note whether it is on or off.

Chapter 5

RESULTS AND DISCUSSION

In this chapter all the results are compiled and the trend of the results is discussed to analyze the behavior of composite sandwich structure at static and dynamic loading.

5.1 Static Tests Results

The specimens have been subjected to loading until failure. The ultimate strength of structure have been recorded.

5.1.1 Load and Displacement behavior

Static tests were carried out to determine the ultimate load and stiffness of the sandwich panel in order to set the amplitude of fatigue loading. The average flexural strength of panel on the basis of static test result is given in table 5.1. The behavior of the load versus the displacement for the monotonic tests is shown in fig. 5.1. Five different phases have been observed during the force and deflection behavior of the sandwich panels.

Phase 1 shows the very small change of load approximate zero with small deflection. The deflection along the span length show the elastic behavior of specimens. Phase 2 shows the linear elastic behavior of panel until the ultimate load is achieved. This show the compressive and tensile behavior of specimens. During Phase 2, the stiffness of panel reduces because of the face yield. Phase 3 shows the abrupt decrease of the load followed by the stiffness degradation of honeycomb because of the small core indentation at the loading area. Phase 4 shows the slightly slow reduction of load corresponding the structural stabilization. Its mean specimen will carry the more load less than maximum failure load with the increase of displacement with time. Phase 5 occurs after the further application of load, load carrying ability of panel reduces and permanent deformation occurred because of the inter laminar shear failure of facing, bending of cell walls and core shear.

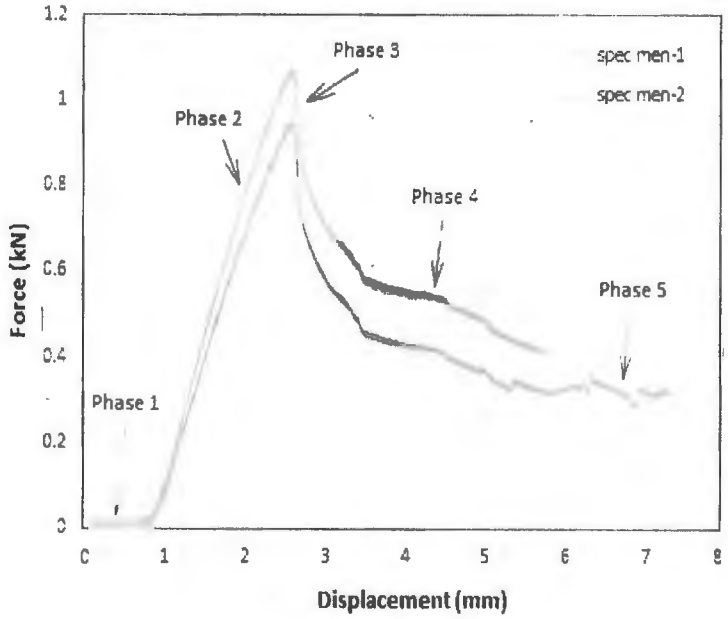

Figure 5.1: Force versus Displacement

Table 5.1: Theoretical calculations of the Average Flexural Strength of Panels

Properties	Core wall Aluminum 5052-H32 Face sheet E-glass fiber
Core Compressive Strength (GPa)	5.67
Face Compressive Strength (MPa)	403
Core Shear Strength (MPa)	1.35
Face Shear Strength (MPa)	0.68
Core Shear Modulus (MPa)	5.67
Bending Strength (MPa)	42
Bending Stiffness (Flexural Rigidity) ($MNmm^2$)	23.6
Shear Stiffness (Shear Rigidity) (KN)	103
Beam deflection (mm)	41.8

5.2 Fatigue test results

5.2.1 Deflection vs. Number of cycles

The graph between Fatigue deflection and the number of cycle at different loading levels is shown in fig. 5. It can be seen from the figure that the deflection is almost constant in the start because of core shear resistance and then increases because of the degradation of stiffness. Initiation of failure is considered where the deflection starts to increase abruptly. The slight increase in defection in the beginning is due to the face yielding. The abrupt increase in deflection is caused by the small indentation and bebonding of honeycomb core and face interface at loading area. It was observed that at higher load the initiation of failure occurs near the final failure because of the face yield and final failure is because of indentation but in case of small load the initiation of failure occur because of face yield as well as delamination below the loading area and final failure occurs because of indentation.

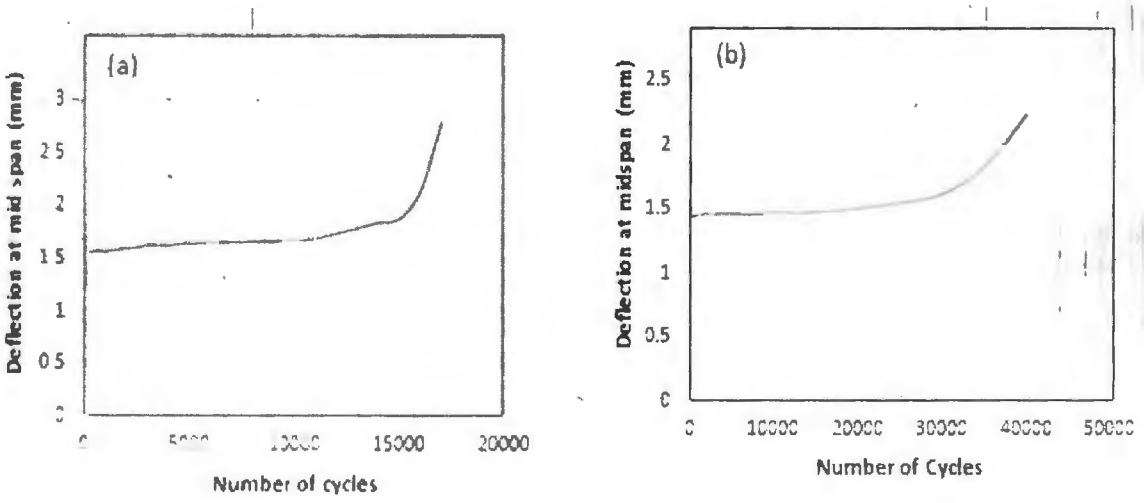

Figure 5.2: Fatigue deflection and number of cycle behavior. (a) Beam deflection at 902N load (b) Beam deflection at 856 N load

5.2.2 Load vs. Number of cycle

The fatigue life is predicted in terms of applied load and number of cycles as shown in fig. 5.3. It has been observed that the fatigue life of sandwich structures increases with the reduction of applied load. So for cyclic loading the specimen is suitable at the 50 to 60% of ultimate load. It has been observed that number of cycles at which initiation of failure of beam starts increases with the decrease of load. The behavior of load level (ratio of applied load to Static failure load) and number of cycles is given in figure 5.3. It was found that at 0.95 loading level the specimen failed

after the 18494 number of cycles. But at 0.90 loading level specimen fails after the 45550 number of cycles. Similarly, at the loading levels 0.85 and 0.80 the failure occurs after 95500 and 215000 number of cycles respectively. In fact at lower loading level the life of sandwich structures increases many times as compared to higher loading levels. And at 0.6 loading level the specimen fails after the millions of cycles.

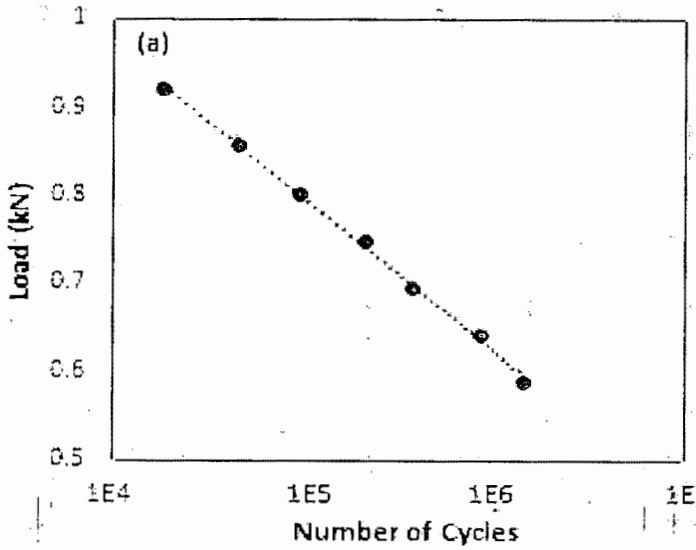

Figure 5.3: Load level and number of cycle response

5.2.3 Bending stress vs. Number of cycle

Bending Stress of beam at different load level is calculated using the equation 3.7. The behavior between Bending stress and number of cycle (S/N curve) is shown in figure 5.4. It has been observed that the bending stress decreases with the increase of number of cycle which show the strength degradation of sandwich structures. It has been observed that number of cycles at which initiation of failure and complete failure of beam starts increases with the decrease of load level. Such as at 37 MPa bending stress the fatigue life of specimen is 18494 number of cycles. But at 35 MPa and 33MPa the life of specimen is 45570 and 95558 number of cycles respectively. This show that by reducing the 2 MPa bending stress the life of panel becomes twice. At 31 MPa the life of panel becomes 215000. It means with the little reduction of applied bending stress life of panel becomes many times.

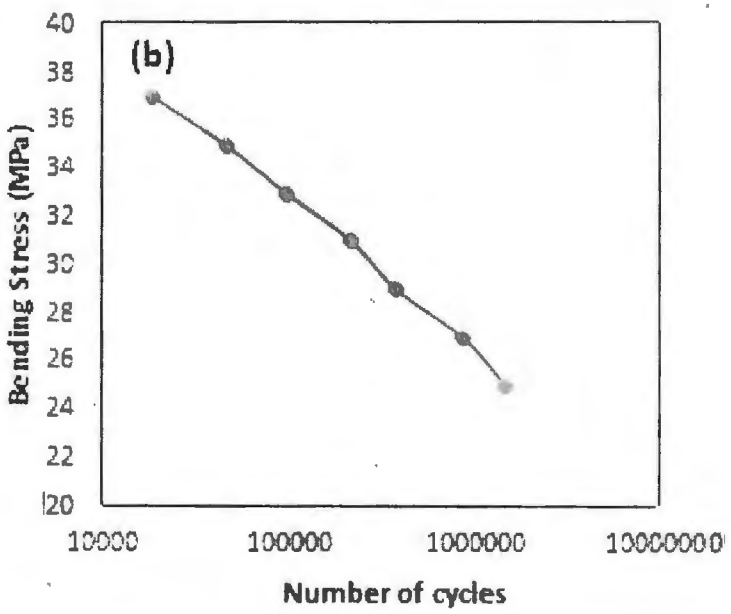

Figure 5.4: Bending stress and number of cycle response

5.3 Failure Modes Studies

Different types of failures modes during experiment have been observed that are verified by SEM analysis.

1. Compression failure of composite facing: In start face sheet compresses when the load increases from the compressive strength of the core as shown in figure 5.5 (a). The magnified image of compressed portion of face sheet is shown in figure 5.5 (b). As a result failure of core indentation have been observed. As a result load carrying ability of panel decreases. Compression failure of face sheet occurs in both monotonic as well as fatigue loading occurs at loading area. It has been observed that the stiffness degradation of panel starts after the compression of core and face sheet.

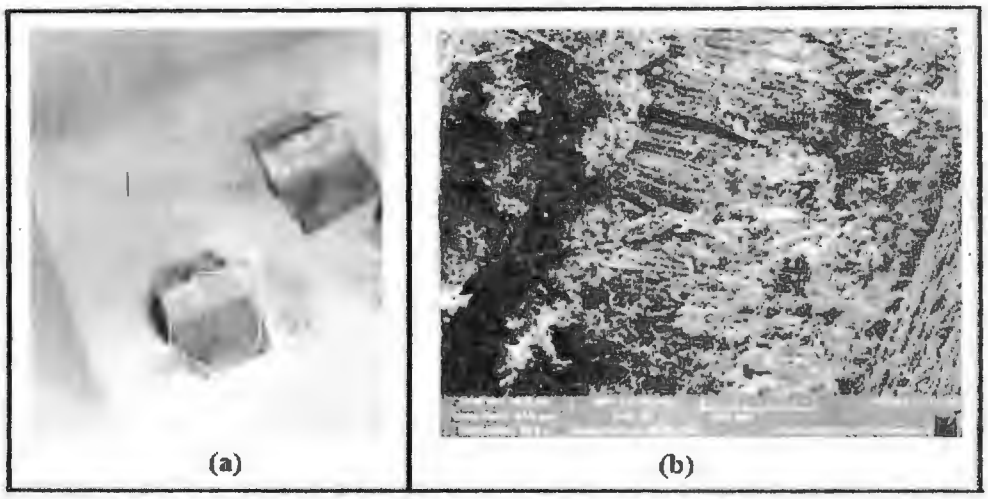

Figure 5.5: Compression of face sheet (a) Skin under observation (b) SEM Image

2. Inter laminar shear failure in facing: The examined portion of specimen is encircled in figure 5.6 (a). The SEM image is magnified at 868 x and view of specific portion is given in figure 5.6 (b). It has been observed that the stiffness degradation of panel starts after the compression of face core and face sheet but further application of load causes the inter laminar shear failure in facing.

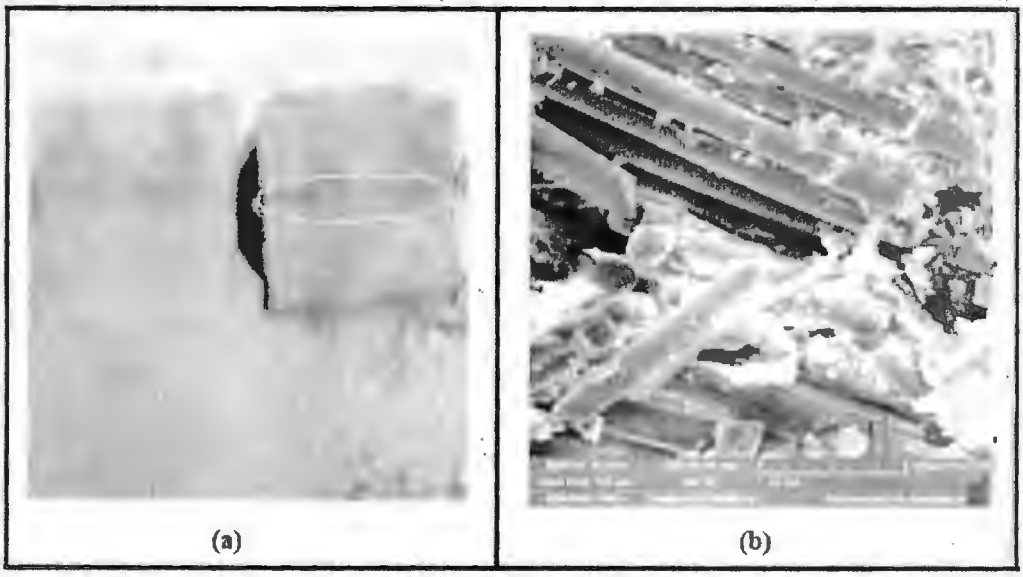

Figure 5.6: Inter laminar shear failure (a) Observed Specimen (b) Magnified SEM Image

3. When the maximum shear strength, in the core increase from the core shear yield strength then the core fails and bending and fracture of cell wall starts. The observed portion is shown in figure 5.7 (a) SEM magnified image of this portion is shown in figure 5.7 (b).

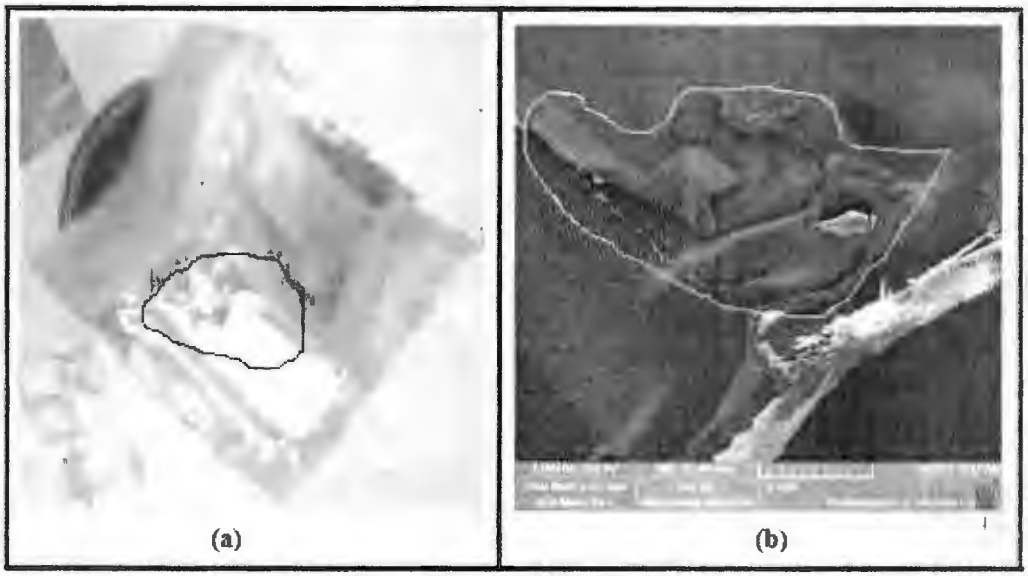

Figure 5.7: Bending of cell wall. (a) Specimen under examination (b) SEM image

4. Interfacial de-bonding was analyzed in the start of failure but it was easily observed after the face yield. The specified portion of interfacial portion and SEM image is shown in figure 5.8.

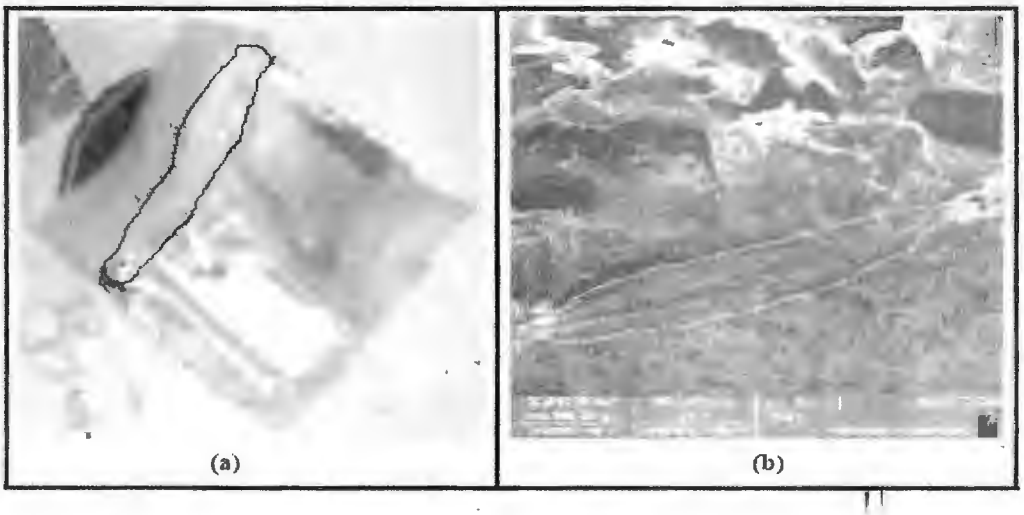

Figure 5.8: Interfacial de-bonding. (a) Face and core bonding (b) SEM image

It has been observed that the initiation of failure of panel in case of both static and fatigue loading occur because of face yield. But the major failure is the core indentation. Also because of further application of loading others defects mentioned above in honeycomb sandwich structures have been observed.

5.4 Discussion of Test Results

5.4.1 Load and Displacement behavior

Static Test result presented in figure 5.1 shows the relationship between load and deflection. The static failure behavior is divided in four phases as mentioned in figure 5.1. The first phase show very small load approximated to zero causes the small deflection that is shown as a horizontal line on the x-axes because of the elastic behavior of sandwich structure. If we compared it with the literature discussed in chapter 2 by Shan-shan Shi [28], Crupi [29], Wahid Boukharouba [10], Abbadi [30], it was found that no one discussed this phase. The reason is that in previous research the data of deflection against the very small load is neglected or it is not recorded precisely. In this research this phase is included to predict the real behavior before the failure. Phase 2 show that with the increase of load displacement increases linearly until the maximum load is achieved because of the compressive and bending strength of core this behavior is verified by Shan-shan shi and Wahid Boukharouba as shown in figure 2.1 (a) and 2.1 (b). The behavior is same because in all cases fabric face sheets have used. But it is little different from the static failure response as shown in figure 2.1 (b) and 2.2 (b). As behavior is not linear until the maximum load. The reason is that in our study the face sheet of glass fabric is used but in cases of figure 2.1 (b) and figure 2.2 (b) face sheets of metal is used. In case of fabric load dropped abruptly after the linear response but in cases of metals after the yield point load also increases and ultimate load is achieved after the yield point.

The 3rd phase shows the drop of load after the strength and stiffness degradation. It is also noted the same response in figure 2.1 and figure 2.2. But it was observed that in figure 2.2 the load is greater as compared to behavior discussed in figure 2.1 and 5.1. The reason is that in case of sandwich structures discussed in figure 2.2 the core of nomex is used. The strength of nomex core is so much less as compared to aluminum core. The 4th phase show that after the drop of load there is little increase of load and a panel again gain a little stabilization because of core shear resistance.

If we compared this phase it was found that similar phase is found in figure 2.1 (a). The similarity in behavior is because of the face sheets of fabric and core of aluminum in both cases.

It is also observed that the total deflection along the span length in figure 2.1 (a) and figure 2.1 (b) is greater as compared to the figure 4.1. The fact is that with the increase of load deflection increases and the further increase of deflection causes the initiation of failure. In both figure 4.1 and 4.8 the deflection of sandwich structure at failure is approximate equal but vary after the failure that this due to the removal of load in this study. But in literature they performed the loading until the complete failure of panel. In such a way Shan-shan Shi considered the more phases after the stabilization which show the variation of load during crack propagation in core.

5.4.2 Deflection vs. Number of cycle

In Fatigue testing the deflection is recorded at different constant amplitude loading level. Deflection versus number of cycle response is plotted in figure 5.2. It was observed that in start deflection remain constant until 20000 of cycles. After that there is little increase of deflection and near about 30000 cycle the deflection increases abruptly. This point is assumed the initiation of failure.

The deflection at mid span and number of cycle response as shown in figure 5.2 is compared with previous data presented by Clark [31] as shown in figures 2.3 . It was found that the behavior is almost similar in start that in both cases the deflection remains constant near about 30000 cycles. But in our study after the 30000 cycles the increase in deflection is slow as compared to Clark [31]. The reason is that the behavior shown in figure 5.2 is for the aluminum honeycomb but the plot shown in figure 2.3 is for aramid honeycomb. In case of aluminum honeycomb after the initial failure there is again a resistance because of core shear resistance of aluminum. On the other hand the core shear resistance made of aramid fiber is less as compared to aluminum.

The data recorded in our study is also compared with F. Cote [32], Samirkumar M. Soni [33] and Abbadi [34] as shown in figure 2.4, figure 2.5 and figure 2.6 (a) respectively. It was found that there is little different from all cases because of different facing and core materials. Because of elastic behavior and good tensile strength of face sheets of aluminum and stainless steel they have more deflection capability and the deflection remains constant and increases rapidly after the degradation. On the other hand in the case face sheets of fiber the deflection increases

slowly because of variation of the compressive strength of face sheets and it increases rapidly after the core indentation or any other expected failure.

5.4.3 Load vs. Number of cycles

In this research work the stiffness degradation and life of composite sandwich structure is also predicted by finding the number of cycle at which initiation of failure occurs at different loading level. The loading level is the ratio of applied load to static failure load. It was found that by decrease of loading level the number of cycle of failure increases. It was found that at 0.95 loading level the specimen failed after the 18494 number of cycles. But at 0.90 loading level specimen fails after the 45000 number of cycles. Similarly, at the loading level the failure occurs after 95158 and 215000 number of cycles respectively. In fact at lower loading level the life of sandwich structures increases. Because of the inadequate facilities we didn't perform the cycle loading at lower loading level. But this increase order shows that the fatigue loading will be suitable almost for the half of static loading.

If we compared it with the behavior of honeycomb having face sheet of aluminum and core of aramid discussed by Abbadi [34] as shown in figure 2.6 (b). It was found that there is so much difference of life of honeycomb in L and W direction. The fatigue life of honeycomb in L direction is so much greater in L direction. In L direction the fatigue life of honeycomb at 0.9 and 0.8 loading level is more than 90000 and 200000 cycles respectively. But at 0.6 loading level the specimen fails after the millions of cycles. The behavior of loading level and number of cycles as shown in figure 5.3 and figure 2.6 (b) is almost similar. But the variation in number of cycles is because of the different flexural strength of composite sandwich structures.

5.4.4 Bending Stress vs. Number of cycles

Life of composite sandwich structures is described by standard S/N curve. The maximum bending stress and number of cycle response at different loading level is shown in figure 5.4. The bending stress is calculated for each constant applied fatigue load. The number of cycle are also find by experimentation as discussed in topic 5.2.2. It was found that with the decrease of bending applied stress the life of sandwich structure increases. At low applied bending stress the life of structure increases many times as compared to higher load level.

[54] Adams, D., and Kuramoto, B. (2012). Damage Tolerance Test Method Development for Sandwich Composites. Technical Review, The University of Utah press.

[55] Mohd, A., and Hafizudin, M. (2016). Simulation Study on Kenaf-Fibre Polyester Composite and LM6 Material. Applied Mechanics and Materials, pp. 584-588.

[56] COMPOSITES, C. (1995). Honeycomb Sandwich Design Technology.

slowly because of variation of the compressive strength of face sheets and it increases rapidly after the core indentation or any other expected failure.

5.4.3 Load vs. Number of cycles

In this research work the stiffness degradation and life of composite sandwich structure is also predicted by finding the number of cycle at which initiation of failure occurs at different loading level. The loading level is the ratio of applied load to static failure load. It was found that by decrease of loading level the number of cycle of failure increases. It was found that at 0.95 loading level the specimen failed after the 18494 number of cycles. But at 0.90 loading level specimen fails after the 45000 number of cycles. Similarly, at the loading level the failure occurs after 95158 and 215000 number of cycles respectively. In fact at lower loading level the life of sandwich structures increases. Because of the inadequate facilities we didn't perform the cycle loading at lower loading level. But this increase order shows that the fatigue loading will be suitable almost for the half of static loading.

If we compared it with the behavior of honeycomb having face sheet of aluminum and core of aramid discussed by Abbadi [34] as shown in figure 2.6 (b). It was found that there is so much difference of life of honeycomb in L and W direction. The fatigue life of honeycomb in L direction is so much greater in L direction. In L direction the fatigue life of honeycomb at 0.9 and 0.8 loading level is more than 90000 and 200000 cycles respectively. But at 0.6 loading level the specimen fails after the millions of cycles. The behavior of loading level and number of cycles as shown in figure 5.3 and figure 2.6 (b) is almost similar. But the variation in number of cycles is because of the different flexural strength of composite sandwich structures.

5.4.4 Bending Stress vs. Number of cycles

Life of composite sandwich structures is described by standard S/N curve. The maximum bending stress and number of cycle response at different loading level is shown in figure 5.4. The bending stress is calculated for each constant applied fatigue load. The number of cycle are also find by experimentation as discussed in topic 5.2.2. It was found that with the decrease of bending applied stress the life of sandwich structure increases. At low applied bending stress the life of structure increases many times as compared to higher load level.

It has been observed that Number of cycles at which initiation of Failure and complete failure of beam starts increases with the decrease of load level. This experimental data of load and number of cycles is used to describe the S-N curve. It was observed that number of cycles increase with the decrease of applied bending stress. Such as at 37 MPa bending stress the fatigue life of specimen is 18494 number of cycles. But at 35 MPa and 37MPa the life of specimen is 45500 and 95158 number of cycles. This show that by reducing the 2 MPa bending stress almost the number of cycle increases two times.

If we compared it with data discussed by Kanny [37] as shown in figure 2.8 it was found that the response is almost same as in both cases there is very small variation of stress with respect to number of cycles. The relationship between bending stress and number of cycle is also verified by Yi-Ming Jen [2] as shown in figure 2.9. The change in plot is because of the least number of samples tested in current research. But Yi-Ming Jen [2] investigated the bending stress response for millions of cycles.

5.4.5 Failure Modes

Different types of failure modes were observed during the static and fatigue loading condition. It was also found that the initiation of failure occur because of the face yield as shown in figure 5.9 (b). The increase in deflection is also the result of face yield. As Banghai Jiang [1] predicted that the initiation of failure of honeycomb under the three point loading occur because of face yield as shown in figure 5.9.

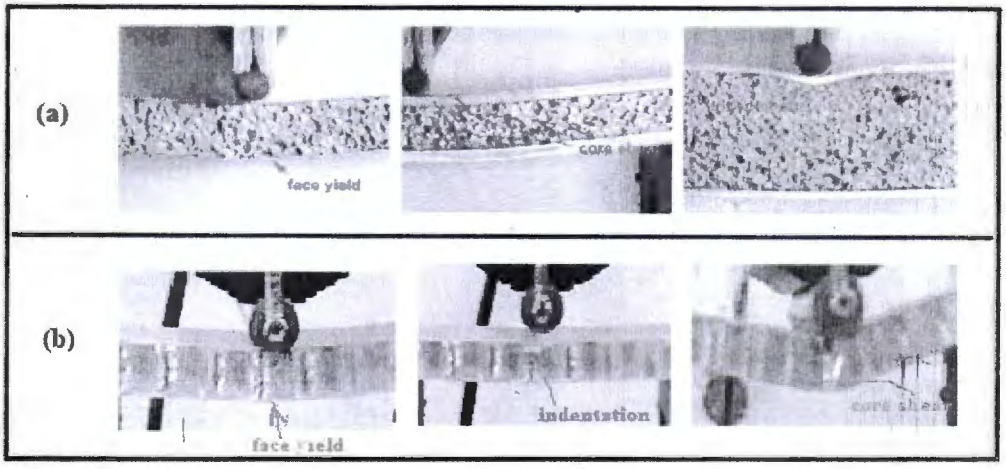

Figure 5.9: Failure modes in 3-point bending loading (a) failure modes observed by Banghai Jiang [1], (b) failure modes observed in current study.

Data Acquisition: Timed
Station Name: force.cfg
Test File Name: benting testing.tst

Running Time Sec	Ch 1 Displacement mm	Ch 1 Force kN
0.144857	-0.96662	-0.40028
7.283366	-1.42612	-0.74113
7.293294	-1.42787	-0.73626
7.303223	-1.42931	-0.74274
7.313151	-1.43113	-0.73692
8.176921	-1.49271	-0.77788
16.87074	-1.02925	-0.44298
16.88066	-1.02235	-0.4303

MTS793|BTW|ENU|1|2|.|/|:|1|0|0|A

Time: 10.2445 Sec ##########

Data Header:
Data Acquisition: Timed
Station Name: force.cfg
Test File Name: benting testing.tst

Running Time Sec	Ch 1 Displacement mm	Ch 1 Force kN
0.144857	-1.0185	-0.46548
0.154785	-1.01887	-0.46092
5.645183	-1.0288	-0.47712
5.655111	-1.03175	-0.48076
7.898926	-1.84139	-0.84532
7.908855	-1.84085	-0.85044
9.348471	-1.39215	-0.73419
9.666179	-1.31148	-0.67579
9.676107	-1.31012	-0.66872
9.686035	-1.30642	-0.67307
11.16574	-1.08113	-0.50818
11.17566	0.26812	-0.4955

[42] Pan, S., Wu, L. (2006). Longitudinal shear strength and failure process of honeycomb cores. Composite Structures, pp. 42-46.

[43] Belingardi, G., Martella, P., and Peroni, L. (2007). Fatigue analysis of honeycomb-composite sandwich beams. Composites Part A: applied science and manufacturing, pp. 1183-1191.

[44] Styles, M., Compston, P., and Kalyanasundaram, S. (2007). The effect of core thickness on the flexural behaviour of aluminium foam sandwich structures. Composite Structures, pp. 532-538.

[45] Jen, Y., and Chang, Y. (2009). Effect of thickness of face sheet on the bending fatigue strength of aluminum honeycomb sandwich beams. Engineering Failure Analysis, pp. 1282-1293.

[46] Zenkert, D., Burman, M. (2009). Failure Mode Shifts in Fatigue of Sandwich Beams. International Conference on Composite Materials.

[47] Manalo, A., Aravinthan, T., Karunasena, W., Islam, M. (2010). Flexural behaviour of structural fibre composite sandwich beams in flatwise and edgewise positions. Composite Structures, pp. 984-995.

[48] Gibson, R. (2010). A mechanics of materials/fracture mechanics analysis of core shear failure in foam core composite sandwich beams. Journal of Sandwich Structures and Materials.

[49] Asokan, P., and Sharma, A. (2010). Recent Advances on Fly ash Particulates and Biofiber Reinforced Lightweight Hybrid Sandwich Composites. International Journal of Engineering Research and Technology press.

[50] Herranen, H., and Pabut. (2012). Design and testing of sandwich structures with different core materials, Materials Science, pp. 45-50.

[51] Zhenkun, L., and Bochang, H. (2014). Flexural effects of sandwich beam with core junctions under in-plane bending. Optics and Lasers in Engineering, pp. 131-139.

[52] Gibson, L., Ashby, M. (1997). Cellular Solids: Structure and Properties, Cambridge university press.

[53] Giglio M., and Manes, A. (2012). Numerical investigation of a three point bending test on sandwich panels with aluminum skins and Nomex™ honeycomb core. Computational Materials Science, pp. 69-78.

It has been observed that Number of cycles at which initiation of Failure and complete failure of beam starts increases with the decrease of load level. This experimental data of load and number of cycles is used to describe the S-N curve. It was observed that number of cycles increase with the decrease of applied bending stress. Such as at 37 MPa bending stress the fatigue life of specimen is 18494 number of cycles. But at 35 MPa and 37MPa the life of specimen is 45500 and 95158 number of cycles. This show that by reducing the 2 MPa bending stress almost the number of cycle increases two times.

If we compared it with data discussed by Kanny [37] as shown in figure 2.8 it was found that the response is almost same as in both cases there is very small variation of stress with respect to number of cycles. The relationship between bending stress and number of cycle is also verified by Yi-Ming Jen [2] as shown in figure 2.9. The change in plot is because of the least number of samples tested in current research. But Yi-Ming Jen [2] investigated the bending stress response for millions of cycles.

5.4.5 Failure Modes

Different types of failure modes were observed during the static and fatigue loading condition. It was also found that the initiation of failure occur because of the face yield as shown in figure 5.9 (b). The increase in deflection is also the result of face yield. As Banghai Jiang [1] predicted that the initiation of failure of honeycomb under the three point loading occur because of face yield as shown in figure 5.9.

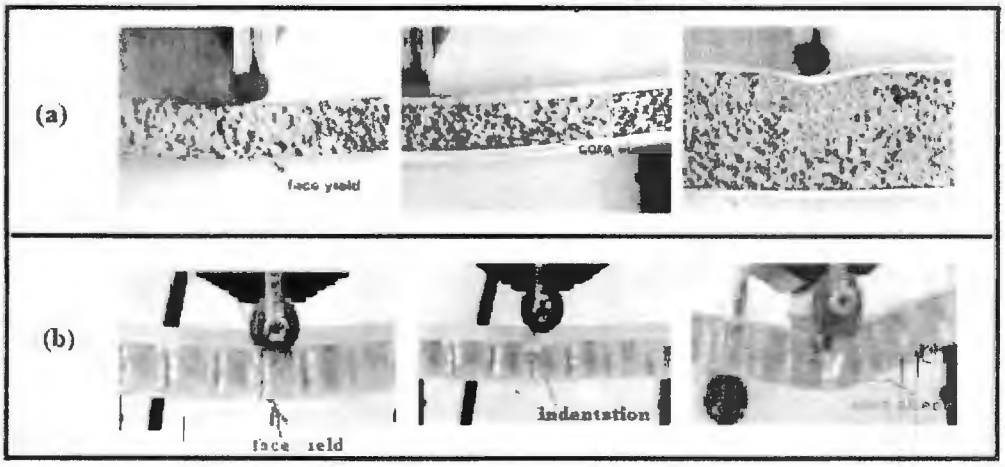

Figure 5.9: Failure modes in 3-point bending loading (a) failure modes observed by Banghai Jiang [1], (b) failure modes observed in current study.

It was discussed that after the initiation of failure the load carrying ability of panel decreases abruptly. This abrupt reduction of stiffness and strength is because of core indentation as shown in figure 5.5 and figure 5.9 (b). This failure mode is also discussed by Banghai Jiang [1], Kalyanasundaram [44] as well as Belouettar [41]. As L.L. Yan, B [39] also predicted that the failure of sandwich structure occurs because of core indentation. The further application of load also causes the other different failure modes such as core shear, the bending and failure of cell walls as shown in figure 5.7 is the indication of core shear. McCormack [26], Belouettar [41], Pan Shi-Dong [42] and Belingardi [43]. Core shear is major mode of failure specially in case of core of web and fabrics as discussed by Zenkert and Burman [46].

Similarly If the load is applied after the failure of beam the interface shear failure of beam and de-bonding of honeycomb and fiber glass interface was also observed using the SEM analysis as shown in figure 5.8 and 5.6 as discussed by Jen and Chang [45], M. Dawood [40]. In fact it was concluded that the observation of several number of specimen that the initiation of failure occur because of the face yield but the failure is the result of core indentation after the several number of cycles.

Analytical model discussed in chapter 3 is also used to predict the failure behavior of composite sandwich structure. By using the mathematical equations 3.13 to 3.18 it was found that only possible failure mode is face yield. But by experimental analysis it was found that face yield is the initial failure mode and other failure modes are observed after the further application of load. So it is concluded that theoretical model is used to predict the only initial failure mode but the real failure behavior is examined by experimentation.

Chapter 6

CONCLUSION OF THIS RESEARCH PRESENTED IN THIS CHAPTER AND FUTURE RECOMMENDATIONS

The research work on the sandwich composite structures is carried out by considering the stiffness degradation producing in the sore of the specimens under three-point bending fatigue loading cycle on the basis of Static Test Results. S/N curve is used to describe the stiffness and strength of composite sandwich structures. Static and Fatigue failure response have been considered. SEM have been used to understand the failure behaviour under different types of loading. The conclusions of the research work are summarized in section 6.1. Future recommendations are presented ins ection 6.2.

6.1 Conclusions

- In static loading, the load and mid span displacement are linearly related.
- The permanent deformation of specimen occurs due to the strength degradation of specimen.
- The Fatigue result show that the fatigue life of the material linearly decreases with stress level
- The initiation of failure occur because of face yield and failure of the specimens is almost due to the core indentation.

6.2 Future Recommendations

This research can be carried out in future considering the following effects: Selection of optimum honeycomb sandwich structure on the bases of flexural rigidity per unit weight and fatigue life.

- Characterizing the damage and fracture for different configuration of honeycomb cells.
- Effect of density and cross sectional area and amount of adhesive used in aluminum honeycomb having fiber glass face sheets.
- Expand 3D DIC technique to a broader range of material analysis.

Appendix

Machine Test data

A. Static Test data

MTS793|BTW|ENU|1|2|.|/|:|1|0|0|A

Data Header:			Time:	10.48633	Sec ##########
Data Acquisition:	Timed				
Station Name:	force.cfg				
Test File Name:	benting testing.tst				
	Ch 1				
Running Time	Displacement	Ch 1 Force			
Sec	mm	kN			
0.14974	-0.00033	0.000631			
0.154785	-0.00026	-0.00133			
0.159831	0.000218	-0.00414			
0.164876	-0.00016	-0.0004			
0.169922	0.000237	-0.00035			
0.174967	0.000571	-0.00506			
0.180013	-0.00018	-0.00382			
3.429362	-0.10801	-0.00034			
3.434408	-0.10871	-0.00277			
6.88558	-0.22353	-0.0083			
6.890625	-0.22457	0.002015			
9.590007	-0.31461	0.000467			
12.5568	-0.41285	-0.00211			
12.56185	-0.41357	-0.00279			
12.5669	-0.41371	0.000412			
12.57194	-0.41402	0.001884			
12.57699	-0.41393	-0.00391			
12.58203	-0.41461	-0.00266			
12.58708	-0.41398	0.000139			
12.59212	-0.41463	0.000477			
12.59717	-0.41442	-0.0044			
12.60221	-0.41589	-0.00635			
12.60726	-0.41406	0.00109			
12.61231	-0.41542	0.001812			
12.61735	-0.41502	-0.00563			
12.6224	-0.41485	-0.0049			

12.62744	-0.41454	-0.00122
12.63249	-0.41586	0.001964
12.63753	-0.41631	-0.00388
12.64258	-0.41522	-0.00563
16.6639	-0.55021	-0.00134
16.66895	-0.54963	-0.00111
16.67399	-0.55053	-0.00255
19.01514	-0.62807	-0.00195
19.02018	-0.62816	0.000995
21.31592	-0.70506	-0.01232
21.32097	-0.70631	-0.01783
24.22217	-0.80166	-0.03682
24.22722	-0.80157	-0.03527
29.61084	-0.98188	-0.15685
31.13965	-1.03234	-0.19231
31.1447	-1.03257	-0.18899
31.14974	-1.03326	-0.1884
31.58871	-1.04775	-0.20021
31.59375	-1.04679	-0.2008
31.80566	-1.05398	-0.20113
32.10336	-1.06498	-0.21386
32.1084	-1.06512	-0.21409
39.52035	-1.31171	-0.38863
40.18132	-1.33273	-0.40695
43.27425	-1.4374	-0.48257
43.2793	-1.43697	-0.48401
47.06348	-1.56299	-0.57085
47.06852	-1.56298	-0.56809
52.61361	-1.74927	-0.68453
52.61865	-1.74781	-0.69159
55.07585	-1.83031	-0.74049
55.08089	-1.83029	-0.73753
55.08594	-1.83053	-0.73968
58.04769	-1.92897	-0.79635
58.05273	-1.92999	-0.7988
58.05778	-1.92978	-0.80348
58.06283	-1.93042	-0.80047
63.47673	-2.10962	-0.89733
63.48177	-2.11047	-0.90147
67.32146	-2.23849	-0.96949
67.3265	-2.23976	-0.9663
67.33154	-2.2393	-0.96876
67.33659	-2.23911	-0.97613

71.23682	-2.36834	-1.02616
71.24187	-2.36956	-1.03308
72.48308	-2.4116	-1.04761
72.48812	-2.41073	-1.04817
75.00586	-2.49453	-1.06049
75.01091	-2.49514	-1.06437
75.01595	-2.49519	-1.0717
75.021	-2.49565	-1.0653
75.02605	-2.4962	-1.05922
75.03109	-2.49639	-1.0633
75.03613	-2.49616	-1.07379
75.04118	-2.49663	-1.06371
76.60531	-2.54796	-0.96137
76.61035	-2.54919	-0.95378
77.14014	-2.5657	-0.90132
77.14519	-2.56561	-0.90192
77.15023	-2.56671	-0.89677
77.15527	-2.56636	-0.9013
77.16032	-2.56684	-0.89735
77.16537	-2.56709	-0.89777
81.14632	-2.69947	-0.79001
81.15137	-2.69979	-0.78648
81.15642	-2.70045	-0.78681
87.82666	-2.92235	-0.69833
87.83171	-2.92178	-0.70454
87.83675	-2.92191	-0.69866
90.92969	-3.02528	-0.67477
90.93474	-3.02517	-0.67434
96.74219	-3.21942	-0.634
96.74724	-3.2203	-0.63583
102.9785	-3.4266	-0.57663
102.9836	-3.42845	-0.57869
102.9886	-3.42682	-0.57924
102.9937	-3.42723	-0.57943
102.9987	-3.4281	-0.57799
110.2795	-3.67029	-0.55985
115.986	-3.86027	-0.5579
115.9911	-3.86099	-0.55354
136.1633	-4.53318	-0.51386
151.5321	-5.04463	-0.45761
151.5371	-5.04488	-0.45906
151.5422	-5.04532	-0.46035
151.5472	-5.04536	-0.45573

151.5523	-5.04601	-0.45705					
151.5573	-5.04625	-0.46159					
Data Header:							
Data Acquisition:	Timed						
Station Name:	force.cfg						
Test File Name:	benting testing.tst						
	Ch 1						
Running Time Sec	Displacement mm	Ch 1 Force kN					
155.1498	-5.168	-0.44744					
155.1548	-5.16656	-0.45079					
155.6392	-5.18215	-0.44489					
155.6442	-5.18192	-0.44565	Time:	165.4857	Sec	##########	
155.6493	-5.18316	-0.44535					
165.9775	-5.52764	-0.41989	Time:	173.7238	Sec	##########	
165.9826	-5.52695	-0.41742					
165.9876	-5.52764	-0.42129					
173.5005	-5.77831	-0.41396					
173.5055	-5.77838	-0.41359					
173.5106	-5.77812	-0.4117					
173.5156	-5.77868	-0.41094					
173.5207	-5.77906	-0.41191					
173.5257	-5.77864	-0.41499					
173.5308	-5.77951	-0.41241					
173.5358	-5.77916	-0.40801					
173.5409	-5.77933	-0.41227					
173.5459	-5.77902	-0.41586					
173.551	-5.77968	-0.41418					
173.556	-5.7797	-0.40841					
173.7074	-5.78495	-0.41436					
173.7124	-5.78462	-0.41119					

B. Fatigue Test data

1. Fatigue Testing at 856 N Load

MTS793|BTW|ENU|1|2|.|/|:|1|0|0|A

Data Header:		Time:	10.58871	Sec	##########	
Data Acquisition:	Timed					
Station Name:	force.cfg					

Test File Name:	benting testing.tst	
Running Time	Ch 1 Displacement	Ch 1 Force
Sec	mm	kN
0.029785	-0.00018	0.00316
0.039714	-0.00026	-0.00483
0.456706	-0.42823	-0.19609
0.466634	-0.44516	-0.2108
0.476563	-0.46045	-0.22032
5.063477	-0.58043	-0.30001
5.073405	-0.58287	-0.30293
5.083334	-0.58636	-0.30076
5.341472	-0.66451	-0.35954
5.3514	-0.66824	-0.37188
5.569824	-0.73702	-0.42237
5.579753	-0.74021	-0.41879
6.354167	-0.9953	-0.59814
6.364095	-0.99796	-0.60245
6.374023	-1.00137	-0.60108
6.383952	-1.00461	-0.60714
7.247722	-1.27723	-0.77904
7.25765	-1.27886	-0.77278
9.153972	-1.36772	-0.81116
9.1639	-1.3651	-0.79381
9.173828	-1.36392	-0.8082
9.183757	-1.36076	-0.7906
9.193686	-1.35923	-0.80627
9.203613	-1.35796	-0.78835
9.77946	-1.2248	-0.70403
9.789389	-1.2231	-0.69318
9.799316	-1.21988	-0.69737
10.12695	-1.12395	-0.63007
10.13688	-1.12251	-0.61769
10.14681	-1.11834	-0.62323
10.15674	-1.11709	-0.6172
10.16667	-1.11286	-0.61964
10.1766	-1.10944	-0.6112
10.18652	-1.10655	-0.61424
10.19645	-1.10343	-0.61083
10.20638	-1.10031	-0.60747
10.21631	-1.0972	-0.60617
10.22624	-1.09447	-0.60096

10.23617	-1.09053	-0.60065
10.24609	-1.0867	-0.59471
10.25602	-1.08428	-0.59899
10.26595	-1.0809	-0.58776
10.27588	-1.07847	-0.59556
10.53402	-0.99317	-0.52846
10.54395	-0.99146	-0.52325
10.55387	-0.98791	-0.52724
10.5638	-0.98443	-0.51937
10.57373	-0.98108	-0.52044

MTS793|BTW|ENU|1|2|.|/|:|1|0|0|A

Data Header: Time: 10.33805 Sec ##########

Data Acquisition: Timed

Station Name: force.cfg

Test File Name: benting testing.tst

Running Time Sec

Ch 1 Displacement mm	Ch 1 Force kN
-0.9442	-0.4737
-0.94417	-0.47209
-1.26037	-0.7062
-1.40994	-0.81148
-1.40814	-0.80663
-1.40678	-0.8099
-1.40504	-0.80351
-1.4037	-0.80971
-1.40239	-0.80022
-1.40069	-0.80599
-1.39819	-0.79768
-1.39766	-0.80323
-1.39663	-0.79882
-1.01067	-0.51304
-1.0073	-0.51233
-1.12816	-0.60052
-1.12451	-0.59508
-0.99691	-0.50391

MTS793|BTW|ENU|1|2|.|/|:|1|0|0|A

Data Header: Time: 10.4445 Sec ##########

Data
Acquisition: Timed
Station Name: force.cfg
Test File Name: benting testing.tst

Running Time Sec	Ch 1 Displacement mm	Ch 1 Force kN
0.144857	-0.96662	-0.40028
7.283366	-1.42612	-0.74113
7.293294	-1.42787	-0.73626
7.303223	-1.42931	-0.74274
7.313151	-1.43113	-0.73692
8.176921	-1.49271	-0.77788
16.87074	-1.02925	-0.44298
16.88066	-1.02235	-0.4303

MTS793|BTW|ENU|1|2|.|/|:|1|0|0|A

10.244

Data Header: Time: 5 Sec ##########
Data
Acquisition: Timed
Station Name: force.cfg
Test File Name: benting testing.tst

Running Time Sec	Ch 1 Displacement mm	Ch 1 Force kN
0.144857	-1.0185	-0.46548
0.154785	-1.01887	-0.46092
5.645183	-1.0288	-0.47712
5.655111	-1.03175	-0.48076
7.898926	-1.84139	-0.84532
7.908855	-1.84085	-0.85044
9.348471	-1.39215	-0.73419
9.666179	-1.31148	-0.67579
9.676107	-1.31012	-0.66872
9.686035	-1.30642	-0.67307
11.16574	-1.08113	-0.50818
11.17566	0.26812	-0.4955

2. Fatigue Testing at 902 N load

MTS793|BTW|ENU|1|2|.|/|:|1|0|0|A

Data Header: Time: 11.3568 Sec

Data Acquisition: Timed

Station Name: force.cfg

Test File Name: benting testing.tst

Running Time Sec	Ch 1 Displacement mm	Ch 1 Force kN
0.029785	-0.10258	-0.04284
3.653646	-0.39611	-0.13276
3.663574	-0.39593	-0.13258
4.586914	-0.55435	-0.25273
4.596843	-0.5567	-0.24958
5.301758	-0.75486	-0.39608
5.311687	-0.75654	-0.4063
5.321615	-0.76046	-0.39852
5.331543	-0.76342	-0.41384
5.976888	-0.97103	-0.55959
5.986816	-0.9749	-0.56231
6.135742	-1.02398	-0.59585
7.118652	-1.34257	-0.79861
7.128581	-1.34501	-0.80107
8.071777	-1.52978	-0.90528
8.081706	-1.5308	-0.9004
8.091635	-1.53108	-0.90639
8.101563	-1.53237	-0.90164
8.111491	-1.53234	-0.90792
8.12142	-1.5327	-0.90241
8.707194	-1.5248	-0.89381
8.717123	-1.52468	-0.89024
8.727051	-1.52356	-0.89475
8.73698	-1.52236	-0.88841
10.45459	-1.12185	-0.59584
10.46452	-1.1196	-0.58692
10.33874	-11.0903	-0.57324
11.3503	-1.08683	-0.56537
11.3568	-1.08348	-0.56644

References

[1] Banghai, J., Zhibin, L., and Fangyun, L. (2015). Failure mechanism of sandwich beams subjected to three-point bending. Composite Structures, pp. 739-745.

[2] Jen, Y., and Chang, L.-Y. (2008). Evaluating bending fatigue strength of aluminum honeycomb sandwich beams using local parameters. International Journal of Fatigue, pp. 1103-1114.

[3] Krzyżak, A., Mazur, M., Gajewski, M., Drozd, K., Komorek, A., and Przybyłek, K. (2016). Sandwich Structured Composites for Aeronautics: Methods of Manufacturing Affecting Some Mechanical Properties. International Journal of Aerospace Engineering.

[4] Allen, H. (2013). Analysis and Design of Structural Sandwich Panels. The Commonwealth and International Library: Structures and Solid Body Mechanics Division, Elsevier.

[5] Petras, A. (1999). Design of sandwich structures. University of Cambridge.

[6] Manshadi, B., Vassilopoulos, A and Keller, K. (2016). Post-wrinkling behavior of webs in GFRP cell-core sandwich structures. Composite Structures, pp. 276-284.

[7] Anjang, A., Chevali, V., Lattimer, B., Case S., Feih, S., and Mouritz, A. (2015). Post-fire mechanical properties of sandwich composite structures. Composite Structures, pp. 1019-1028.

[8] Daniel, I., Ishai, O. (1994). Engineering mechanics of composite materials. Oxford university press.

[9] Rocca S., and Nanni, S. (2005). Mechanical characterization of sandwich structure comprised of glass fiber reinforced core. Composites in Construction, pp. 11-13.

[10] Boukharouba, W., Bezazi, A., and Scarpa, F. (2014). Identification and prediction of cyclic fatigue behaviour in sandwich panels, Measurement. pp. 161-170.

[11] Allen, H. (1969). Analysis and design of structural sandwich panels. Pergamon Press.

[12] Xu, G.-d., Yang, F., Zeng, S., Cheng., & Wang, Z.-H. (2016). Bending behavior of graded corrugated truss core composite sandwich beams. Composite structures, 342-351.

[13] Gholami, M., Alashti, A., & Fathi, A. (2016). Optimal design of a Honeycomb core composite sandwich panel using evolutionary optimization algorithms. Composite Structures, 254-262.

[14] Sadowski, T. (2007). Multiscale modelling of damage and fracture processes in composite materials, Springer Science & Business Media.

[15] Kreja, I. (2011). A literature review on computational models for laminated composite and sandwich panels. Open Engineering, pp. 59-80.

[16] Gibson, F. (2016). Principles of composite material mechanics. CRC press.

[17] Plantema, F. (1966). Sandwich construction, New York, Wiley press.

[18] Zenkert, D. (1995). An introduction to sandwich construction: Engineering materials advisory services.

[19] Triantafillou, T and Gibson, L. (1987). Failure mode maps for foam core sandwich beams," Materials Science and Engineering. pp. 37-53.

[20] Gibson, L., (1984). Optimization of stiffness in sandwich beams with rigid foam cores. Materials Science and Engineering, pp. 125-135.

[21] Mercado, L. (1999). On the response of a sandwich panel with a bilinear core. Mechanics of Composite Materials and Structures, pp. 57-67.

[22] Frostig, Y., and Baruch, M. (1996). Localized load effects in high-order bending of sandwich panels with flexible core. Journal of Engineering Mechanics, pp. 1069-1076.

[23] Timoshenko, S., and Goodier, J., (1970). The ory of Elas tic ity. New York, McGraw-Hill press.

[24] Gibson, L., and Ashby, M. (1999). Cellular solids: structure and properties: Cambridge university press.

[25] Daniel, I., and Gdoutos, E. (2002). Failure modes of composite sandwich beams," International Journal of Damage Mechanics. pp. 309-334.

[26] McCormack, T., Miller, R., and Gibson, L. (2001). Failure of sandwich beams with metallic foam cores," International Journal of Solids and Structures. pp. 4901-4920.

[27] Kulkarni, N., Mahfuz, H., Jeelani, S., and Carlsson, L. (2003). Fatigue crack growth and life prediction of foam core sandwich composites under flexural loading," Composite Structures. pp. 499-505.

[28] Shi, S.-S., Sun, X.-Z., Hu., & Chen, H.-R. (2014). Carbon-fiber and aluminum-honeycomb sandwich composites with and without Kevlar-fiber interfacial toughening. (67 vol.). Composites Part A: Applied Science and Manufacturing, pp. 102-110.

[29] Crupi, V., Epasto, G., and Guglielmino, E. (2013). Comparison of aluminium sandwiches for lightweight ship structures: honeycomb vs. foam. (13 vol.). Marine Structures, 74-96.

[30] Abbadi, A., Tixier, C., Gilgert, J., & Azari, Z. (2015). Experimental study on the fatigue behaviour of honeycomb sandwich panels with artificial defects. Composite Structures, 394-405.

[31] Clark, S., Shenoi, R., & Allen, H. (1999). Modelling the fatigue behaviour of sandwich beams under monotonic, 2-step and block-loading regimes. (vol. 59). Composites science and technology, 471-486.

[32] Côté, F., Fleck, N. and Deshpande. (2007). Fatigue performance of sandwich beams with a pyramidal core. International journal of fatigue, pp. 1402-1412.

[33] Soni, M., Gibson, R., and Ayorinde, E. (2009). The influence of subzero temperatures on fatigue behavior of composite sandwich structures. Composites Science and Technology, pp. 829-838.

[34] Abbadi, A., Azari, Z, Belouettar, S., and Freres, P. (2010). Modelling the fatigue behaviour of composites honeycomb materials (aluminium/aramide fibre core) using four-point bending tests. International Journal of Fatigue. pp. 1739-1747.

[35] Burman M., and Zenkert, D. (1997). Fatigue of foam core sandwich beams—1: undamaged specimens, International journal of fatigue, pp. 551-561.

[36] Burman M., and Zenkert, D. (1997). Fatigue of foam core sandwich beams—2: effect of initial damage, International journal of fatigue, pp. 563-578.

[37] Kanny, K., and Mahfuz, M. (2005). Flexural fatigue characteristics of sandwich structures at different loading frequencies. Composite Structures, pp. 403-410.

[38] Cunningham, P., and White, R. (2001). A new measurement technique for the estimation of core shear strain in closed sandwich structures. Composite structures, pp. 319-334.

[39] Yan, L., and Han, B. (2014). Three-point bending of sandwich beams with aluminum foam-filled corrugated cores. Materials & Design, pp. 510-519.

[40] Dawood, M., and Taylor, E. (2010). Static and fatigue bending behavior of pultruded GFRP sandwich panels with through-thickness fiber insertions. Composites Part B: Engineering, pp. 363-374.

[41] Belouettar, S., and Abbadi, A. (2009). Experimental investigation of static and fatigue behaviour of composites honeycomb materials using four point bending tests. Composite Structures, pp. 265-273.

[42] Pan, S., Wu, L. (2006). Longitudinal shear strength and failure process of honeycomb cores. Composite Structures, pp. 42-46.

[43] Belingardi, G., Martella, P., and Peroni, L. (2007). Fatigue analysis of honeycomb-composite sandwich beams. Composites Part A: applied science and manufacturing, pp. 1183-1191.

[44] Styles, M., Compston, P., and Kalyanasundaram, S. (2007). The effect of core thickness on the flexural behaviour of aluminium foam sandwich structures. Composite Structures, pp. 532-538.

[45] Jen, Y., and Chang, Y. (2009). Effect of thickness of face sheet on the bending fatigue strength of aluminum honeycomb sandwich beams. Engineering Failure Analysis, pp. 1282-1293.

[46] Zenkert, D., Burman, M. (2009). Failure Mode Shifts in Fatigue of Sandwich Beams. International Conference on Composite Materials.

[47] Manalo, A., Aravinthan, T., Karunasena, W., Islam, M. (2010). Flexural behaviour of structural fibre composite sandwich beams in flatwise and edgewise positions. Composite Structures, pp. 984-995.

[48] Gibson, R. (2010). A mechanics of materials/fracture mechanics analysis of core shear failure in foam core composite sandwich beams. Journal of Sandwich Structures and Materials.

[49] Asokan, P., and Sharma, A. (2010). Recent Advances on Fly ash Particulates and Biofiber Reinforced Lightweight Hybrid Sandwich Composites. International Journal of Engineering Research and Technology press.

[50] Herranen, H., and Pabut. (2012). Design and testing of sandwich structures with different core materials, Materials Science, pp. 45-50.

[51] Zhenkun, L., and Bochang, H. (2014). Flexural effects of sandwich beam with core junctions under in-plane bending. Optics and Lasers in Engineering, pp. 131-139.

[52] Gibson, L., Ashby, M. (1997). Cellular Solids: Structure and Properties, Cambridge university press.

[53] Giglio M., and Manes, A. (2012). Numerical investigation of a three point bending test on sandwich panels with aluminum skins and Nomex™ honeycomb core. Computational Materials Science, pp. 69-78.

[54] Adams, D., and Kuramoto, B. (2012). Damage Tolerance Test Method Development for Sandwich Composites. Technical Review, The University of Utah press.

[55] Mohd, A., and Hafizudin, M. (2016). Simulation Study on Kenaf-Fibre Polyester Composite and LM6 Material. Applied Mechanics and Materials, pp. 584-588.

[56] COMPOSITES, C. (1995). Honeycomb Sandwich Design Technology.